The Joint and Product Meta Distributions of the SIR and Their Applications to Secrecy and Cooperation

Xinlei Yu, Qimei Cui, *Senior Member, IEEE*, Yuanjie Wang, and Martin Haenggi, *Fellow, IEEE*

***Abstract*—The meta distribution (MD) of the signal-to-interference ratio (SIR) provides more fine-grained information about the link performance than the standard success probability. This paper focuses on a fundamental extension of the SIR MD—the joint MD of the SIR at different locations, and studies its applications to physical layer security and cooperative reception. The concept of the joint MD of the SIR is formally introduced for two or more users (locations), as well as the joint conditional success probability and the n-th order product MD, which is a simpler version of the joint MD. The joint MD is first applied to physical layer security. The network reliability of the secrecy transmission based on the MD is studied, taking into account the signal and interference correlations between the legitimate user and the eavesdropper. Next the joint MD is applied to cooperative reception, where we consider the scenario that the base station sends a message to a group of users, and the goal is that at least one user successfully receives the message. The moments of the conditional probability of the event that the transmission succeeds at at least one of the two users are derived. The results demonstrate the practical relevance of the joint MD.**

***Index Terms*—Meta distribution, joint probability, interference correlation, stochastic geometry, physical layer security, cooperative reception, Poisson point process.**

I. Introduction

A. Motivation

Due to the rapid improvement of the cellular networks technology in recent years, future cellular networks will be more and more diverse and heterogeneous in order to meet a variety of user demands in mobile data rate and emerging applications and services [2]. Stochastic geometry has emerged as an important mathematical method in the modeling and analysis of cellular networks in recent few years [3]–[5]. The standard success probability $\mathbb{P}(\text{SIR} > \tau)$, i.e., the complementary cumulative distribution function (CCDF) of the signal-to-interference ratio (SIR) at the typical user, is the main performance metric in most of the literature. However, it does not provide information on the individual link performances. To address this shortcoming, the meta distribution (MD) was recently introduced in [6]. The MD of the SIR provides more fine-grained information by characterizing the entire distribution of the link performances. For example, the SIR MD answers the question—"For a certain transmission rate, what fraction of links achieve a given target reliability?". So far, the MD was defined only for a single user. To address scenarios involving multiple users, an extension of the concept to multiple users or locations is necessary. This is the goal of this paper.

Manuscript date March 20, 2020.

Part of this work has been presented at the 2018 IEEE Global Communications Conference (GLOBECOM'18) [1].

The work was supported in part by the National Natural Science Foundation of China under Grant 61941114, 61971066, 61941105 and 61471058, in part by the Beijing Natural Science Foundation under Grant L182038, in part by the National Youth Top-notch Talent Support Program, in part by the 111 Project of China under Grant B16006, and in part by the BUPT Excellent Ph.D. Students Foundation under Grant CX2018205. *(Corresponding author: Qimei Cui.)*

Xinlei Yu and Qimei Cui are with the National Engineering Laboratory for Mobile Network Technologies, Beijing University of Posts and Telecommunications, Beijing 100876, China (e-mail: xinleiyu@hotmail.com, cuiqimei@bupt.edu.cn).

Yuanjie Wang is with the National Computer Network Emergency Response Technical Team/Coordination Center of China (CNCERT/CC), Beijing 100029, China (e-mail: wang.yuanjie@outlook.com).

Martin Haenggi is with the Dept. of Electrical Engineering, University of Notre Dame, IN, 46556, USA (e-mail: mhaenggi@nd.edu).

B. Related Work

The MD of the SIR is first introduced in [6] and calculated for Poisson bipolar and cellular networks. As a key step, the b-th moments of the conditional success probability given the point process are derived. The first and second moments are used to obtain a simple beta distribution approximation, which is shown to be very accurate. Most of the prior work on the MD is restricted to a single user/location. The MD for device-to-device (D2D) underlay and the local delay are given in [7]. In [8], the MD for millimeter wave communication in the D2D scenario and the MD of the transmission rate are analyzed, and a general beta distribution as a modified approximation is proposed. [9] considers two types of users, namely the typical general user and the typical cell-corner user, in the downlink coordinated multipoint transmission/reception (CoMP) including joint transmission and dynamic point blanking, and dynamic point selection/dynamic point blanking, and calculates the MD of the SIR. [10] studies the MD of the secrecy rate in physical layer security jointly considering multiple users—both the legitimate user and the colluding/non-colluding eavesdropper, but ignores the interference.

Recently, there has been some work on the joint performance of two or more users/locations, but only for the standard success (coverage) probability. [11] provides an analytical framework for the joint coverage probability (although not for the MD) at two spatial locations in a cellular network based on the handoff rate and coverage analysis model in [12], where the two users are served by their nearest base stations (BSs). However, this exact analysis is cumbersome since for each value of the distance v between the two users, the probabilities of same-BS and different-BS association need to be considered. [13] proposes optimization schemes of the transmit power for the users in Poisson clustered out-of-band D2D networks based on the joint coverage probability of a cluster,

while the joint coverage probability is obtained by multiplying the coverage probability of each pair of users in a cluster, i.e., assuming independence for each pair of users. [14], [15] study the joint uplink-downlink rate or SINR coverage probability for heterogeneous cellular networks (HCNs) and cellular-based RF-powered internet of thing (IoT) networks. The authors consider the success probability for both uplink and downlink jointly. In [16], the authors consider the joint signal to interference plus noise ratio (SINR) success probability of all antennas in a MIMO receiver in downlink MIMO HCNs. [17] analyzes the joint success probability of the SINR for Type-I hybrid automatic repeat request (HARQ) users in different time slots in HCNs where the BSs are spatially correlated. In [18], the authors quantify the effect of spatial interference correlation on opportunistic secure spectrum access in cellular networks. It is an application of the joint success probability at two different locations. Our prior conference paper [1] focuses on an application of the MD of the joint conditional SIR distribution to a problem in physical layer security. In this paper, we focus on the underlying fundamental mathematical problem and give a general definition and approach for the joint MD of the SIR.

C. Contributions and Paper Organization

In this paper, we fundamentally extend the concept of the SIR MD to the joint MD of the SIR at multiple locations and study its applications to physical layer security and cooperation.

The contributions of this paper are summarized as follows:

- The concept of the joint MD of the SIR is introduced for two or more users (locations). Specifically, we formally define the joint conditional success probability, the n-th order joint MD, and the n-th order product MD, which is a simpler version of the joint MD.
- We consider both one-dimensional (1D) and two-dimensional (2D) Poisson network models with two users that are associated with the same BS, to study the joint SIR performance of two users. This BS association scenario corresponds to the two applications to physical layer security and cooperation. The moments of the joint conditional success probability are derived for both 1D and 2D network models in order to obtain the product MD.
- We focus on the distribution of the distance from two users to their (common) serving BS and closest interferer in the 2D Poisson network. The probability distribution functions (PDFs) of these distances are derived, and some properties are revealed.
- We study the application to physical layer security. The typical legitimate user and a nearby eavesdropper are considered. Through analytical derivations and simulations, we give the opportunistic conditional secure spectrum access probability and its distribution. We also obtain the reliability of the network when different levels of security are required and explore the effect of the distance between legitimate user and eavesdropper on the reliability.
- We study the application to cooperative reception. We consider the scenario that the BS sends a message to a group of users, and the goal is that at least one user successfully receives the message. The first and second moments of the conditional probability for the event that the transmission succeeds at at least one of two users are derived.

The remainder of the paper is organized as follows. Sec. II introduces the standard MD and its beta approximation and presents the definitions for the joint and product MD. Sec. III introduces the 1D and 2D Poisson network models and studies some properties of the product MD. Sec. IV and Sec. V apply the analysis framework to physical layer security and cooperative reception, respectively. Sec. VI concludes the paper.

II. Joint and Product Meta Distribution

In this section, we define the joint and product SIR MD to analyze the SIR performance for two or more users at different locations jointly. Before, we review the definition of the standard (single-user) SIR MD.

A. Meta Distribution and its Beta Approximation

The MD of the SIR, introduced in [6], is defined as the CCDF of the random variable

$$P_{\mathrm{s}}(\tau) \triangleq \mathbb{P}\left(\mathrm{SIR} > \tau \mid \Phi\right), \tag{1}$$

which is the conditional success probability given the point process Φ. Hence, the MD is formally given by

$$\bar{F}(\tau,\nu) \triangleq \mathbb{P}\left(P_{\mathrm{s}}(\tau) > \nu\right), \quad \nu \in [0,1], \tag{2}$$

where $\mathbb{P}$ here is the probability measure of the point process Φ. It is quite likely impossible to calculate the MD directly from the definition in (2), hence it is obtained indirectly from the moments of $P_{\mathrm{s}}(\tau)$. The b-th moment of $P_{\mathrm{s}}(\tau)$ is denoted by

$$\begin{aligned} M_b &\triangleq \mathbb{E}\left(P_{\mathrm{s}}(\tau)^b\right) = \int_0^1 \nu^b \mathrm{d}F_{P_{\mathrm{s}}}(\nu) \\ &= \int_0^1 b\nu^{b-1}\bar{F}_{P_{\mathrm{s}}}(\nu)\mathrm{d}\nu, \quad b \in \mathbb{C}, \end{aligned} \tag{3}$$

where the notation $\bar{F}_{P_{\mathrm{s}}}(\nu)$ is also used for the MD $\bar{F}(\tau,\nu)$, and $F_{P_{\mathrm{s}}}(\nu) = 1-\bar{F}_{P_{\mathrm{s}}}(\nu)$. It is noteworthy that the standard success probability captures only the mean of $P_{\mathrm{s}}(\tau)$, i.e., $p_{\mathrm{s}}(\tau) \equiv M_1$, while the MD is the distribution of the conditional success probability $P_{\mathrm{s}}(\tau)$.

The b-th moments of $P_{\mathrm{s}}(\tau)$ for downlink Poisson cellular networks are given by [6, Thm. 2] as

$$M_b = \frac{1}{{}_2F_1(b,-\delta;1-\delta;-\tau)}, \quad b \in \mathbb{C}, \tag{4}$$

where ${}_2F_1(\cdot)$ is the Gaussian hypergeometric function.

The exact MD can then be obtained from the integer moments $M_j = \mathbb{E}(P_{\mathrm{s}}(\tau)^j)$, $j \in \{0\} \cup \mathbb{N}$, as [19]

$$\bar{F}_{P_{\mathrm{s}}}(\nu) = 1 - \lim_{i\to\infty} \sum_{k=0}^{\lfloor i\nu \rfloor} \sum_{j=k}^{i} \binom{i}{j}\binom{j}{k}(-1)^{j-k} M_j, \ \nu \in (0,1], \tag{5}$$

and $\bar{F}_{P_\mathrm{s}}(0) = 1$, where $\lfloor u \rfloor$ is the largest integer smaller than or equal to u.

Alternatively, it is natural and often sufficient to approximate the MD by matching its first and second moment M_1 and M_2 to the beta distribution, resulting in

$$\bar{F}_{P_\mathrm{s}}(\nu) \approx 1 - I_\nu\Big(\frac{M_1\beta}{1-M_1}, \beta\Big), \tag{6}$$

$$I_\nu(a,b) = \frac{\int_0^\nu t^{a-1}(1-t)^{b-1}\mathrm{d}t}{B(a,b)},\ \beta = \frac{(M_1-M_2)(1-M_1)}{M_2-M_1^2}, \tag{7}$$

where $I_\nu(a,b)$ is the cumulative distribution function (CDF) of the beta distribution, i.e., the regularized incomplete beta function with shape parameters $a, b > 0$, and $B(a,b)$ is the beta function. This approximation has been shown to be rather accurate [6], [9].

B. Definitions

We consider a general system model where BSs form a general stationary and ergodic point process $\Phi \subset \mathbb{R}^d$. The vector $\mathbf{x} = (x_1, x_2, \ldots, x_n) \in (\mathbb{R}^d)^n$ is a (deterministic) vector of n user locations. The SIR at the i-th location x_i is defined as

$$\mathrm{SIR}_i \triangleq \frac{h_{x_i,s(x_i)}\ell(x_i - s(x_i))}{\sum_{z\in\Phi\setminus\{s(x_i)\}} h_{x_i,z}\ell(x_i - z)}, \tag{8}$$

where $s(x_i) \in \Phi$ is the BS serving location x_i, $h_{u,v}$ is the fading between u and v where $h_{u,v}$ is independent of $h_{u',v'}$ if $\{u,v\} \neq \{u',v'\}$ and also independent of Φ, and ℓ is the path loss law. For nearest-BS association, $s(x_i) = \arg\min\{z \in \Phi\colon \|z - x_i\|\}$.

We first define the joint conditional success probability at n locations.

Definition 1 (Joint conditional success probability) *The n-th order joint conditional success probability is the joint distribution of the SIRs at locations $\mathbf{x} = (x_1, x_2, \ldots, x_n)$ given the point process Φ, i.e.,*

$$P_\mathrm{s}^{(n)}(\mathbf{x}, \boldsymbol{\tau}) \triangleq \mathbb{P}\Big(\bigcap_{i=1}^n \{\mathrm{SIR}_i > \tau_i\} \mid \Phi\Big) \overset{(a)}{=} \prod_{i=1}^n \mathbb{P}(\mathrm{SIR}_i > \tau_i \mid \Phi) = \prod_{i=1}^n P_i(\tau_i), \tag{9}$$

where $\boldsymbol{\tau} = (\tau_1, \tau_2, \ldots, \tau_n) \in (\mathbb{R}^+)^n$ is the threshold vector of the conditional success probability at the n locations, $P_i(\tau_i) \triangleq \mathbb{P}(\mathrm{SIR}_i > \tau_i \mid \Phi)$ is the conditional success probability at the i-th location x_i, and (a) follows from the independence of the fading coefficients $h_{u,v}$[1].

Next we proceed to the joint MD of the SIR.

[1]Given the point process Φ, the remaining randomness of SIR_i is the set of fading coefficients. Because of the independence of the fading coefficients, the SIR_i are conditionally independent.

Definition 2 (n-th order joint MD of the SIR) *The n-th order joint MD of the SIR is the joint distribution of the conditional success probability at locations $\mathbf{x} = (x_1, x_2, \ldots, x_n)$, i.e.,*

$$\bar{F}_\mathrm{j}^{(n)}(\mathbf{x}, \boldsymbol{\tau}, \boldsymbol{\nu}) \triangleq \mathbb{P}\Big(\bigcap_{i=1}^n \{\mathbb{P}(\mathrm{SIR}_i > \tau_i \mid \Phi) > \nu_i\}\Big) = \mathbb{P}\Big(\bigcap_{i=1}^n \{P_i(\tau_i) > \nu_i\}\Big), \tag{10}$$

where $\boldsymbol{\nu} = (\nu_1, \nu_2, \ldots, \nu_n) \in [0,1]^n$ is the reliability vector at the n locations, and $\boldsymbol{\tau} = (\tau_1, \tau_2, \ldots, \tau_n)$.

A simpler version of the joint MD is called the *product MD*. It is defined as follows.

Definition 3 (n-th order product MD of the SIR) *The n-th order product MD of the SIR is the distribution of the joint conditional success probability at locations $\mathbf{x} = (x_1, x_2, \ldots, x_n)$, i.e.,*

$$\bar{F}^{(n)}(\mathbf{x}, \boldsymbol{\tau}, \nu) \triangleq \mathbb{P}\big(P_\mathrm{s}^{(n)}(\mathbf{x}, \boldsymbol{\tau}) > \nu\big) = \mathbb{P}\Big(\mathbb{P}\Big(\bigcap_{i=1}^n \{\mathrm{SIR}_i > \tau_i\} \mid \Phi\Big) > \nu\Big) = \mathbb{P}\Big(\prod_{i=1}^n P_i(\tau_i) > \nu\Big), \quad \nu \in [0,1], \tag{11}$$

where $\boldsymbol{\tau} = (\tau_1, \tau_2, \ldots, \tau_n)$.

The key difference between Def. 2 and 3 is that the product MD is the CCDF of the joint conditional success probability $P_\mathrm{s}^{(n)}(\mathbf{x}, \boldsymbol{\tau})$, while the joint MD is the joint distribution of the conditional success probabilities $P_i(\tau_i)$, $i = 1, \ldots, n$. For $n = 1$, they both correspond to $\mathbb{P}(P_1(\tau_1) > \nu_1)$, i.e., the MD of a single user.

We can obtain the product MD (11) from the PDF of the joint MD (10):

$$\begin{aligned}\bar{F}^{(n)}(\mathbf{x}, \boldsymbol{\tau}, \nu) &= \mathbb{P}\Big(\prod_{i=1}^n P_i(\tau_i) > \nu\Big) \\ &= 1 - \mathbb{E}\left(\mathbb{P}\left(P_1(\tau_1) \le \frac{\nu}{\prod_{i=2}^n P_i(\tau_i)} \mid P_2(\tau_2), \ldots, P_n(\tau_n)\right)\right) \\ &= 1 - \int_0^1 \cdots \int_0^1 \mathrm{d}\nu_2 \cdots \mathrm{d}\nu_n \\ &\quad \cdot \int_0^{\frac{\nu}{\prod_{i=2}^n \nu_i}} f_{P_1(\tau_1),\ldots,P_n(\tau_n)}(\nu_1, \nu_2, \ldots, \nu_n)\,\mathrm{d}\nu_1, \end{aligned} \tag{12}$$

where $f_{P_1(\tau_1),\ldots,P_n(\tau_n)}(\nu_1, \nu_2, \ldots, \nu_n)$ is the PDF of the joint MD of the SIR (10). We use the product MD as the main performance metric in the rest of the paper.

To distinguish the standard MD from the joint MD, we use the notation $M_b^{(n)}$ for the moments of the joint conditional success probability of the users at n locations. The formal definition of $M_b^{(n)}$ is given here.

Definition 4 (Moments of the joint conditional success probability) *The b-th moment of the joint conditional success*

probability $P_{\mathrm{s}}^{(n)}(\mathbf{x},\boldsymbol{\tau})$ *at locations* $\mathbf{x}=(x_1,x_2,\ldots,x_n)$ *is given by*

$$\begin{aligned} M_b^{(n)}(\mathbf{x}) &\triangleq \mathbb{E}\big(\big(P_{\mathrm{s}}^{(n)}(\mathbf{x},\boldsymbol{\tau})\big)^b\big) \\ &= \mathbb{E}\bigg(\bigg(\mathbb{P}\Big(\bigcap_{i=1}^{n}\{\mathrm{SIR}_i>\tau_i\}\mid\Phi\Big)\bigg)^b\bigg) \\ &= \mathbb{E}\bigg(\prod_{i=1}^{n}P_i^b(\tau_i)\bigg), \end{aligned} \tag{13}$$

where $\boldsymbol{\tau}=(\tau_1,\tau_2,\ldots,\tau_n)$.

It is noteworthy that $M_b^{(1)}$ is the standard moment in (3), and $M_b^{(2)}$ is the moment of the joint conditional success probability at two locations ($n=2$).

Let $\Psi=\{u_1,u_2,\ldots\}\subset\mathbb{R}^d$ be a stationary and ergodic point process of users. Then the n-th order joint MD of the SIR gives the fraction of users u_k for which the following holds: The conditional probability that the SIR at $u_k+(x_i-x_1)$ exceeds τ_i is higher than ν_i, for each $i=1,2,\ldots,n$. The n-th order product MD of the SIR gives the fraction of users for which the following holds: The joint conditional probability for the n events that the SIR at $u_k+(x_i-x_1)$ exceeds τ_i for each $i=1,2,\ldots,n$, i.e., by the conditional independence, the product of the n conditional probabilities that the SIR at $u_k+(x_i-x_1)$ exceeds τ_i, is higher than ν.

III. The Product Meta Distribution in Poisson Networks

In this section, we study some properties of the product MD in Poisson networks. The joint and product MDs extend the scope of the MD framework to important applications in secrecy (Sec. IV) and cooperation (Sec. V). In the rest of this paper, we mostly focus on the case $n=2$. Due to the motion-invariance of the model, for $n=2$, $\bar{F}^{(2)}(\mathbf{x},\boldsymbol{\tau},\nu)\equiv\bar{F}^{(2)}(v,\boldsymbol{\tau},\nu)$, where $\mathbf{x}=(x_1,x_2)$ and $v=\|x_1-x_2\|$. This simplification is analogous to the one frequently applied for second moment measures and pair correlation functions [20, Def. 6.6].

A. System Model

1) 2D Network Model: The BSs are distributed according to a homogeneous Poisson point process (PPP) $\Phi\subset\mathbb{R}^2$ of intensity λ. We consider two users—UE1 located on the origin $o\triangleq(0,0)$ and UE2 located on $(v,0)$, i.e., the location vector is $\mathbf{x}=(o,(v,0))$. Assuming that both UEs connect to the nearest BS to UE1 (the origin) and attempt to receive the message from it in the same time slot, the location of this serving BS is $s(o)=s((v,0))=\arg\min\{z\in\Phi\colon\|z-o\|\}$. UE2 may lie in the same Voronoi cell as UE1 or another cell. This BS association scenario (in contrast to the one where both users connect to their nearest BS) is the one relevant for the two applications to physical layer security and cooperation. A realization of this network model is shown in Fig. 1. The BSs are always active, and Rayleigh fading and the standard path loss law with path loss exponent $\alpha>2$ are adopted, i.e., the channel gain between the receiver x and the transmitter z can be expressed as $h_{x,z}\|x-z\|^{-\alpha}$, where $h_{x,z}$ is i.i.d. exponential

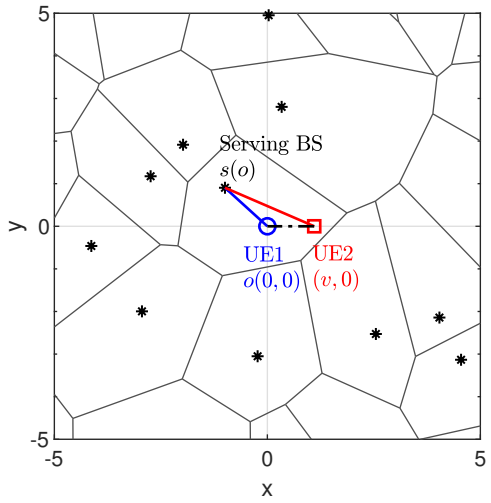

Fig. 1. A realization of the 2D network model for BS density $\lambda=0.1$. The star markers represent the BSs and the circle marker represents the typical user named UE1 at the origin o. UE1 is associated to the nearest BS. The line connecting the star marker and the circle marker indicates the downlink signal link of UE1. The square marker represents UE2 at $(v,0)$. UE2 is also associated to UE1's BS, and UE1 and UE2 both receive the message from it at the same time slot. The line connecting the star marker and the square marker indicates the downlink signal link of UE2.

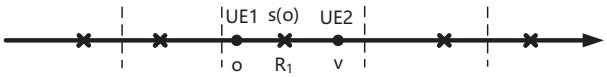

Fig. 2. A realization of the 1D network model. The star markers represent the BSs, the circle marker represents the typical user UE1 at the origin o and UE2 at v. The dashed lines are the cell boundaries. UE1 is associated to the nearest BS $s(o)$ at R_1, and UE2's serving BS is also $s(o)$.

with unit mean. The effect of thermal noise is neglected. We denote the distance between UE1 and its serving BS as $R_1\triangleq\|s(o)\|$, and the distance between UE2 and its serving BS (which is the same as UE1's) as $R_2\triangleq\|s(o)-(v,0)\|$.

Then the SIRs (8) can be expressed as

$$\mathrm{SIR}_1=\frac{h_{o,s(o)}R_1^{-\alpha}}{\sum\limits_{z\in\Phi\setminus\{s(o)\}}h_{o,z}\|z\|^{-\alpha}}, \tag{14}$$

$$\mathrm{SIR}_2=\frac{h_{(v,0),s(o)}R_2^{-\alpha}}{\sum\limits_{z\in\Phi\setminus\{s(o)\}}h_{(v,0),z}\|(v,0)-z\|^{-\alpha}}. \tag{15}$$

2) 1D Network Model: We also consider a 1D network model, which is more tractable and leads to insights that also apply to 2D models. This simpler case has its own application scenario, e.g., for vehicular networks [21]–[25]. In this 1D network model, the BSs are distributed according to a homogeneous PPP $\Phi\subset\mathbb{R}$ of intensity λ. UE1 and UE2 are placed at o and $v\geq0$, respectively, i.e., the locations are $\mathbf{x}=(o,v)$. As in the 2D case, UE1 and UE2 both connect to the nearest BS to UE1 (the origin), therefore the serving BS is located at either $s(o)=-R_1$ or $s(o)=R_1$. A realization of this 1D network model is shown in Fig. 2. The channel fading and the path loss law are the same as in the 2D case.

It is noteworthy that these 1D and 2D PPP models have the potential to apply to arbitrary models with strong shadowing

under certain conditions. [26] recently explored the impact of strong shadowing (with or without moderate spatial correlation) on network models. For the standard MD, the following holds: If the BS association takes shadowing into account (as it usually does), then with strong enough shadowing, any point process looks like a PPP from the point of view of the typical user. In other words, using strongest-BS association with strong shadowing in an arbitrary point process (where "strongest" includes path loss and shadowing) is equivalent to nearest-BS association in a PPP (without shadowing or with shadowing, here it makes no difference). So shadowing is incorporated by the fact that we use a Poisson model. For the joint or product MD, we can expect this result to hold if the distances between the locations are small relative to the mean nearest-neighbor distance of the BSs. For $n = 2$, this means that $v \ll 1/\sqrt{\lambda}$.

B. Moments of the Joint Conditional Success Probability

For arbitrary point processes Φ, the conditional success probability at the i-th location x_i can be expressed as

$$P_i(\tau_i) = \prod_{z\in\Phi\setminus\{s(o)\}} \frac{1}{1+\tau_i \frac{\|x_i - s(o)\|^\alpha}{\|x_i - z\|^\alpha}}. \tag{16}$$

Then, the b-th moments of the second-order joint conditional success probability for both 1D and 2D Poisson networks are given as follows. We analyze the the 1D case first due to its superior tractability.

1) 1D Poisson Networks: For 1D Poisson networks, the PDF of the link distance R_1 between UE1 and its serving BS can be obtained from the void probability of PPP as

$$f_{R_1}^{\text{1D}}(r) = 2\lambda \exp\left(-2\lambda r\right). \tag{17}$$

Theorem 1 *The b-th moment $M_b^{(2)}(v)$ of the joint conditional success probability for 1D Poisson networks is*

$$M_b^{(2)}(v) = \int_0^\infty \exp\big(Q(1,1)+Q(1,-1)\big)\exp\left(-2\lambda r\right)\lambda \mathrm{d}r + \int_0^\infty \exp\big(Q(-1,1)+Q(-1,-1)\big)\exp\left(-2\lambda r\right)\lambda \mathrm{d}r,\ b\in\mathbb{C}, \tag{18}$$

where

$$Q(p,q) = -\int_r^\infty \left(1 - \frac{\left(1+\tau_1\frac{r^\alpha}{z^\alpha}\right)^{-b}}{\left(1+\tau_2\frac{|v-pr|^\alpha}{|v-qz|^\alpha}\right)^b}\right)\lambda \mathrm{d}z,\ p,q\in\{-1,1\}. \tag{19}$$

Proof: For 1D Poisson networks, the distances from the BSs to UE2 can be written as $R_2 = \|v - s(o)\| = |v \pm R_1|$, and $\|v - z\| = |v \pm z|$. Using (16), the b-th moment for the joint conditional success probability of UE1 and UE2 in 1D Poisson networks is

$$\begin{aligned}
M_b^{(2)}(v) &= \mathbb{E}(P_1^b(\tau_1)P_2^b(\tau_2)) \\
&= \mathbb{E}\bigg(\prod_{z\in\Phi\setminus\{s(o)\}} \left(\frac{1}{1+\frac{\tau_1 R_1^\alpha}{\|z\|^\alpha}}\right)^b \left(\frac{1}{1+\frac{\tau_2\|v-s(o)\|^\alpha}{\|v-z\|^\alpha}}\right)^b\bigg) \\
&\overset{(a)}{=} \mathbb{E}_{R_1}\bigg(\exp\bigg(-\int_{R_1}^\infty \bigg(1 - \frac{\left(1+\tau_1\frac{R_1^\alpha}{\|z\|^\alpha}\right)^{-b}}{\left(1+\tau_2\frac{\|v-s(o)\|^\alpha}{\|v-z\|^\alpha}\right)^b}\bigg)2\lambda \mathrm{d}z\bigg)\bigg) \\
&= \mathbb{E}_{R_1}\bigg(\exp\bigg(-\int_{R_1}^\infty \bigg(1 - \frac{\left(1+\tau_1\frac{{R_1}^\alpha}{z^\alpha}\right)^{-b}}{\left(1+\tau_2\frac{|v\pm R_1|^\alpha}{|v\pm z|^\alpha}\right)^b}\bigg)2\lambda \mathrm{d}z\bigg)\bigg) \\
&\overset{(b)}{=} \frac{1}{2}\int_0^\infty \exp\bigg(-\frac{1}{2}\int_r^\infty \bigg(1 - \frac{\left(1+\tau_1\frac{r^\alpha}{z^\alpha}\right)^{-b}}{\left(1+\tau_2\frac{|v-r|^\alpha}{|v-z|^\alpha}\right)^b}\bigg)2\lambda \mathrm{d}z \\
&\quad - \frac{1}{2}\int_r^\infty \bigg(1 - \frac{\left(1+\tau_1\frac{r^\alpha}{z^\alpha}\right)^{-b}}{\left(1+\tau_2\frac{|v-r|^\alpha}{(v+z)^\alpha}\right)^b}\bigg)2\lambda \mathrm{d}z\bigg) f_{R_1}^{\text{1D}}(r)\mathrm{d}r \\
&\quad + \frac{1}{2}\int_0^\infty \exp\bigg(-\frac{1}{2}\int_r^\infty \bigg(1 - \frac{\left(1+\tau_1\frac{r^\alpha}{z^\alpha}\right)^{-b}}{\left(1+\tau_2\frac{(v+r)^\alpha}{|v-z|^\alpha}\right)^b}\bigg)2\lambda \mathrm{d}z \\
&\quad - \frac{1}{2}\int_r^\infty \bigg(1 - \frac{\left(1+\tau_1\frac{r^\alpha}{z^\alpha}\right)^{-b}}{\left(1+\tau_2\frac{(v+r)^\alpha}{(v+z)^\alpha}\right)^b}\bigg)2\lambda \mathrm{d}z\bigg) f_{R_1}^{\text{1D}}(r)\mathrm{d}r,
\end{aligned} \tag{20}$$

where (a) employs the probability generating functional (PGFL) of the PPP [20, Thm. 4.9], (b) uses the law of total probability. ■

2) 2D Poisson Networks: For 2D Poisson networks, the PDF of the link distance R_1 between UE1 and its serving BS can be obtained from the void probability of PPP as

$$f_{R_1}(r) = 2\pi\lambda r \exp\left(-\pi\lambda r^2\right). \tag{21}$$

Theorem 2 *The b-th moment $M_b^{(2)}(v)$ of the joint conditional success probability for 2D Poisson networks is*

$$M_b^{(2)}(v) = \int_0^{2\pi}\int_0^\infty \frac{f_{R_1}(r)}{2\pi}\exp\bigg(-\int_0^{2\pi}\int_r^\infty \lambda z \cdot \bigg(1 - \frac{\left(1+\tau_1 r^\alpha z^{-\alpha}\right)^{-b}}{\left(1+\tau_2\left(\frac{r^2+v^2-2rv\cos\theta}{z^2+v^2-2zv\cos\omega}\right)^{\frac{\alpha}{2}}\right)^b}\bigg)\mathrm{d}z\mathrm{d}\omega\bigg)\mathrm{d}r\mathrm{d}\theta,\ b\in\mathbb{C}. \tag{22}$$

Proof: From (16), the b-th moment for the joint conditional success probability of UE1 and UE2 is

$$\begin{aligned}
M_b^{(2)}(v) &= \mathbb{E}(P_1^b(\tau_1)P_2^b(\tau_2)) \\
&= \mathbb{E}\bigg(\prod_{z\in\Phi\setminus\{s(o)\}} \left(\frac{1}{1+\frac{\tau_1 R_1^\alpha}{\|z\|^\alpha}}\right)^b \left(\frac{1}{1+\frac{\tau_2\|(v,0)-s(o)\|^\alpha}{\|(v,0)-z\|^\alpha}}\right)^b\bigg) \\
&\overset{(a)}{=} \mathbb{E}_{R_1,\Theta}\bigg(\exp\bigg(-\int_0^{2\pi}\int_{R_1}^\infty \lambda z \cdot \bigg(1 - \frac{\left(1+\tau_1 R_1^\alpha z^{-\alpha}\right)^{-b}}{\left(1+\tau_2\left(\frac{R_1^2+v^2-2R_1v\cos\Theta}{z^2+v^2-2zv\cos\omega}\right)^{\frac{\alpha}{2}}\right)^b}\bigg)\mathrm{d}z\mathrm{d}\omega\bigg)\bigg) \\
&\overset{(b)}{=} \int_0^{2\pi}\int_0^\infty \frac{f_{R_1}(r)}{2\pi}\exp\bigg(-\int_0^{2\pi}\int_r^\infty \lambda z
\end{aligned}$$

$$\cdot\left(1-\frac{\left(1+\tau_1 r^{\alpha} z^{-\alpha}\right)^{-b}}{\left(1+\tau_2\left(\frac{r^2+v^2-2rv\cos\theta}{z^2+v^2-2zv\cos\omega}\right)^{\frac{\alpha}{2}}\right)^{b}}\right)\mathrm{d}z\mathrm{d}\omega\Bigg)\mathrm{d}r\mathrm{d}\theta, \quad (23)$$

where (a) employs the PGFL of the PPP [20, Thm. 4.9] and uses the polar coordinates $s(o) = (R_1\cos\Theta, R_1\sin\Theta)$, and (b) uses the PDFs of R_1 and Θ in 2D Poisson networks to take the expectation over R_1 and Θ. ∎

Remark 1 (The b-th moment for independent SIRs): If the SIRs are assumed independent for UE1 and UE2, the b-th moment is given by

$$\begin{aligned}\tilde{M}_b^{(2)}(v) &= \mathbb{E}(\mathbb{P}(\mathrm{SIR}_1 > \tau_1 \mid \Phi)^b)\mathbb{E}(\mathbb{P}(\mathrm{SIR}_2 > \tau_2 \mid \Phi)^b) \\ &= M_b(\tau_1)M_b'(\tau_2), \end{aligned} \quad (24)$$

where $M_b(\tau_1)$ given in (4) and

$$M_b'(\tau_2) = \int_0^{2\pi}\int_0^{\infty} \frac{f_{R_1}(r)}{2\pi}\exp\Bigg(-\int_0^{2\pi}\int_r^{\infty}\lambda z \cdot\left(1-\left(1+\tau_2\left(\frac{r^2+v^2-2rv\cos\theta}{z^2+v^2-2zv\cos\omega}\right)^{\frac{\alpha}{2}}\right)^{-b}\right)\mathrm{d}z\mathrm{d}\omega\Bigg)\mathrm{d}r\mathrm{d}\theta \quad (25)$$

are the b-th moments for UE1 and UE2, respectively. The two SIRs are not identically distributed since the serving BS is the one closest to the origin (UE1), which is not necessarily the one closest to UE2.

3) Moments for n Locations: Here we assume that n UEs are located on a line at $x_i = (v_i, 0)$ for 2D Poisson networks, or $x_i = v_i$ for 1D Poisson networks, where $i = 1, \ldots, n$, with $v_1 = 0$ and $v_i > 0$ $(i = 2, \ldots, n)$.

Corollary 1 (The moment for n locations) *The b-th moment of the n-order joint conditional success probability for 1D Poisson networks is*

$$\begin{aligned}M_b^{(n)}(\boldsymbol{v}) &= \int_0^{\infty}\exp\left(Q'(1,1)+Q'(1,-1)\right)\exp\left(-2\lambda r\right)\lambda\mathrm{d}r \\ &+\int_0^{\infty}\exp\left(Q'(-1,1)+Q'(-1,-1)\right)\exp\left(-2\lambda r\right)\lambda\mathrm{d}r,\ b\in\mathbb{C},\end{aligned} \quad (26)$$

where $\boldsymbol{v} = (v_1, v_2, \ldots, v_n)$, and

$$Q'(p,q) = -\int_r^{\infty}\left(1-\frac{\left(1+\tau_1 r^{\alpha} z^{-\alpha}\right)^{-b}}{\prod_{i=2}^{n}\left(1+\tau_2\frac{|v_i-pr|^{\alpha}}{|v_i-qz|^{\alpha}}\right)^{b}}\right)\lambda\mathrm{d}z, \quad p,q\in\{-1,1\}. \quad (27)$$

For 2D Poisson networks, it is

$$M_b^{(n)}(\boldsymbol{v}) = \int_0^{2\pi}\int_0^{\infty}\frac{f_{R_1}(r)}{2\pi}\exp\Bigg(-\int_0^{2\pi}\int_r^{\infty}\lambda z \cdot\left(1-\frac{\left(1+\tau_1 r^{\alpha} z^{-\alpha}\right)^{-b}}{\prod_{i=2}^{n}\left(1+\tau_2\left(\frac{r^2+v_i^2-2rv_i\cos\theta}{z^2+v_i^2-2zv_i\cos\omega}\right)^{\frac{\alpha}{2}}\right)^{b}}\right)\mathrm{d}z\mathrm{d}\omega\Bigg)\mathrm{d}r\mathrm{d}\theta, \quad b\in\mathbb{C}. \quad (28)$$

Proof: It is straightforward to generalize Theorem 1 and 2 to n locations. ∎

C. Distance Distribution

In order to further analyze the effect of distance v on the SIR performance, we next focus on the distribution of the distances of UE1 and UE2 to their closest interferer and serving BS. We denote the distance between UE1 and its closest interferer as $R_1' \triangleq \min_{z\in\Phi\setminus\{s(o)\}}\|z\|$, and the distance between UE2 and its closest interferer as $R_2' \triangleq \min_{z\in\Phi\setminus\{s(o)\}}\|z-(v,0)\|$. The 2D Poisson network model is considered in this subsection.

The PDF $f_{R_1}(r)$ of the distance R_1 of UE1 to its serving BS is given in (21), and the distribution of the distance R_1' of UE1 to its closest interferer is

$$f_{R_1'}(r) = 2\pi\lambda r(\pi\lambda r^2)\exp\left(-\pi\lambda r^2\right), \quad (29)$$

which is the distance from the origin to its second-nearest point in a PPP.

Next we find an approximation of the PDF of the distance R_2' of UE2 to its closest interferer. When $v = 0$, the distribution of the distance R_2' is the standard nearest-interferer distribution, i.e., the PDF of R_2' is the same as that of R_1', given in (29), with mean

$$\mathbb{E}(R_2') = \frac{3}{4\sqrt{\lambda}}, \quad v = 0. \quad (30)$$

When $v\to\infty$, the distribution of R_2' approaches the empty space function of the PPP which is the Rayleigh distribution with mean

$$\mathbb{E}(R_2') = \frac{1}{2\sqrt{\lambda}}, \quad v\to\infty, \quad (31)$$

i.e., the PDF of R_2' is the same as that of R_1 given in (21). As shown in Fig. 3(a), with increasing v the PDFs gradually change from (29) to (21). It is natural to use the mean of R_2' to approximate the PDF of R_2' parameterized by v. According to the forms of (30) and (31), the prototype function $\mathbb{E}(R_2') = \frac{3+av^c}{(4+2av^c)\sqrt{\lambda}}$ is used. Using the Curve Fitting Toolbox of Matlab to fit the simulation results, the best fitting coefficients are $a = 12.95$ $(11.9, 14)$, $c = 2.938$ $(2.808, 3.068)$ with 95% confidence bounds. Rounding the coefficients, we set $a = 12$, $c = 3$, and the fitting results are shown in Fig. 4. Hence, we obtain an approximation of the PDF of R_2'.

Lemma 1 *The PDF of R_2' parameterized by v is tightly approximated by*

$$f_{R_2'}(r) \approx \frac{2\pi\lambda r\exp\left(-\pi\lambda r^2\right)(\pi\lambda r^2+6v^3)}{6v^3+1} \quad (32)$$

with the mean $\mathbb{E}(R_2') = \frac{3+12v^3}{(4+24v^3)\sqrt{\lambda}}$.

The approximated results of the PDF for R_2' with $\lambda = 1$ calculated from (32) are shown in Fig. 3(a) and compared with their simulation results.

Next, we focus on the distribution of the distance R_2 from UE2 at $(v, 0)$ to the serving BS $s(o)$. We can directly obtain the exact expression of this random variable from the definition of the Ricean distribution in 2D plane.

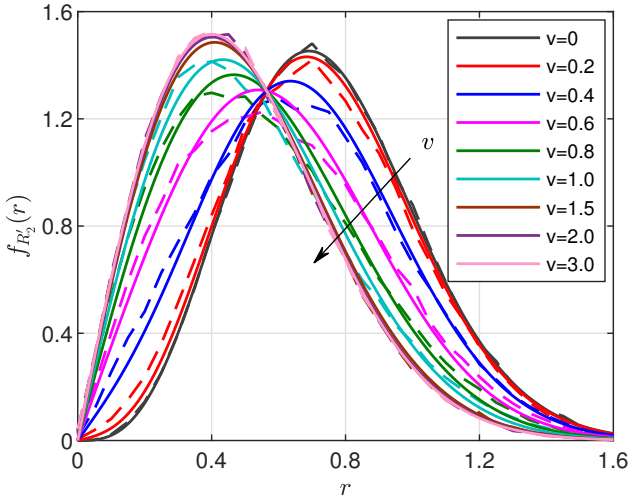

(a) R_2'—UE2 to its closest interferer

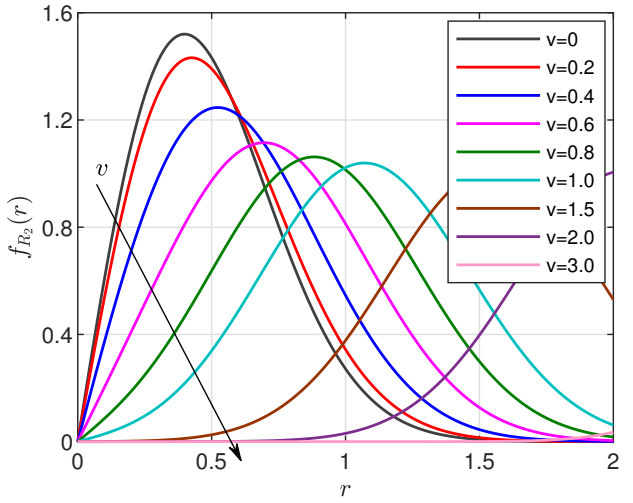

(b) R_2—UE2 to its serving BS

Fig. 3. The PDF of the distance of UE2 to its serving BS and the closest interferer with $\lambda = 1$. $v = 0, 0.2, 0.4, 0.6, 0.8, 1, 1.5, 2.0, 3.0$ is increasing along the arrows. The solid lines in (a) are the analytical approximations from (32), the dashed lines in (a) are the simulation results, and the solid lines in (b) are the exact analytical results from (33).

Lemma 2 *The PDF of R_2 is the Ricean distribution with parameters v and $\sigma = \frac{1}{\sqrt{2\pi\lambda}}$, i.e.,*

$$f_{R_2}(r) = \frac{r}{\sigma^2}\exp\Big(\frac{-(r^2+v^2)}{2\sigma^2}\Big)I_0\Big(\frac{rv}{\sigma^2}\Big) = 2\pi\lambda r\exp\big(-\pi\lambda(r^2+v^2)\big)I_0\big(2\pi\lambda rv\big), \quad (33)$$

where $I_0(z)$ is the modified Bessel function of the first kind with order zero.

The mean of R_2 is $\mathbb{E}(R_2) = \sigma\sqrt{\frac{\pi}{2}}L_{1/2}(-\frac{v^2}{2\sigma^2}) = \frac{1}{2\sqrt{\lambda}}L_{1/2}(-\pi\lambda v^2)$, and the variance of R_2 is $\mathrm{Var}(R_2) = 2\sigma^2+v^2-\frac{\pi\sigma^2}{2}L_{1/2}^2(\frac{-v^2}{2\sigma^2}) = \frac{1}{\pi\lambda}+v^2-\frac{1}{4\lambda}L_{1/2}^2(-\pi\lambda v^2)$, where $L_{1/2}(z)$ denotes the Laguerre polynomial with parameter $1/2$. Fig. 5 shows the analytical results of the mean and variance of R_2 for $\lambda = 1$. It is observed from Fig. 5 that as $v \to \infty$, the mean approaches v, and the variance approaches $\frac{1}{2\pi\lambda} \approx 0.16$.

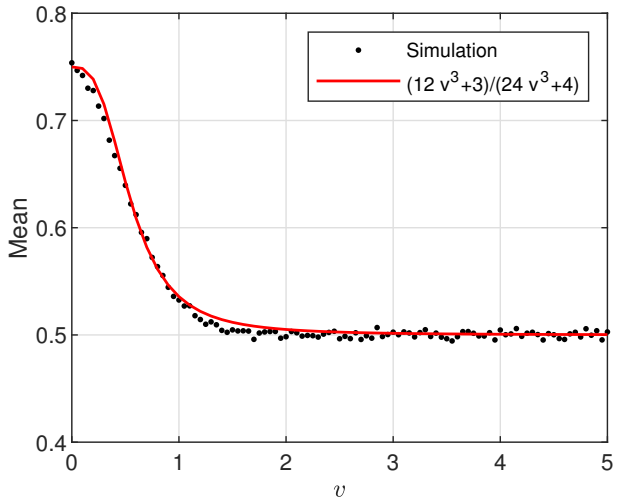

Fig. 4. The simulated mean of the distance R_2' of UE2 to its closest interferer and its approximation (32) with $\lambda = 1$.

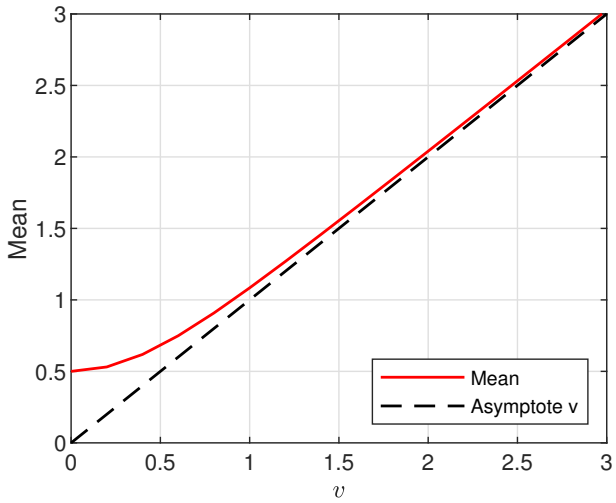

(a) Mean $\mathbb{E}(R_2)$

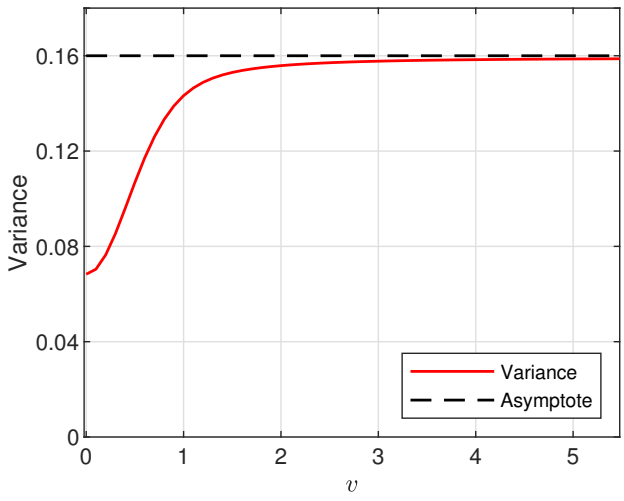

(b) Variance $\mathrm{Var}(R_2)$

Fig. 5. The analytical results for the mean and variance of the distance R_2 of UE2 to its serving BS with $\lambda = 1$. The dashed line in (a) is the asymptote v, and the dashed line in (b) is the asymptote $\frac{1}{2\pi}$.

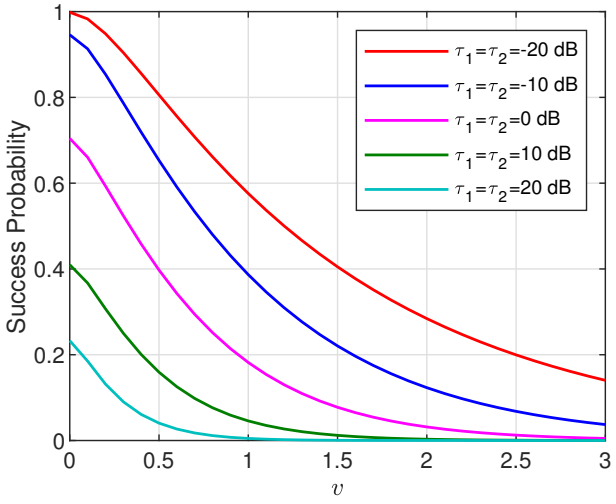

(a) Joint Success Probability $M_1^{(2)}$

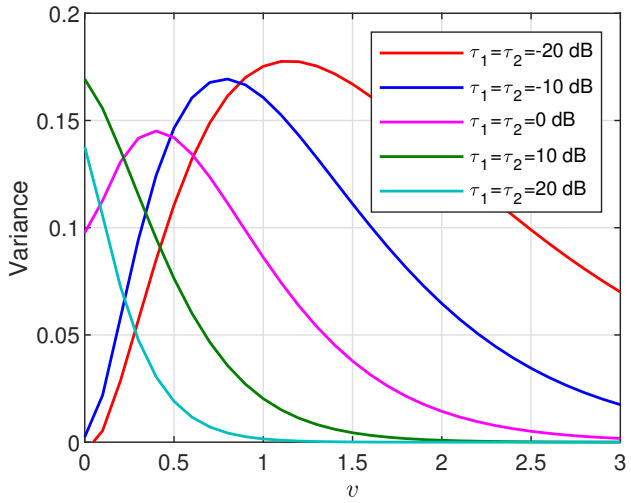

(b) Variance $M_2^{(2)} - (M_1^{(2)})^2$

Fig. 6. The success probability $M_1^{(2)}$ and the variance $M_2^{(2)} - (M_1^{(2)})^2$ for 1D Poisson networks.

The PDF for R_2 with $\lambda = 1$ calculated from (33) is shown in Fig. 3(b).

Based on this insight, we can give a qualitative analysis of the SIR performance. The change of v does not affect SIR_1, but SIR_2. As v increases, the mean of the distance R_2 of UE2 to its serving BS increases and approaches v, while the mean of the distance R_2' of UE2 to its closest interferer tends to a constant. Therefore, for relatively large v, the distance R_2 becomes the main factor affecting SIR_2. The regions of interest thus have the smaller values of v, which we will mostly focus on, in the numerical results.

D. Numerical Results

Here we show numerical and simulation results for both 1D and 2D Poisson network models. The intensity of the BSs in this section is set to $\lambda = 1$. The path loss exponent is $\alpha = 4$. Here and in the rest of the paper, we use the beta approximation, obtained from the first and second

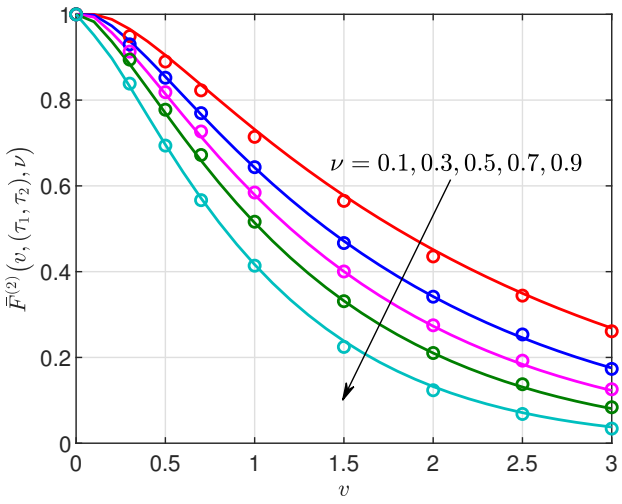

(a) $\tau_1 = \tau_2 = -20$ dB

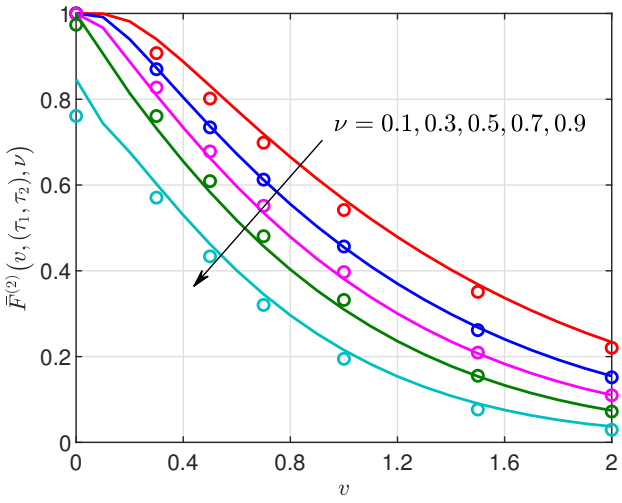

(b) $\tau_1 = \tau_2 = -10$ dB

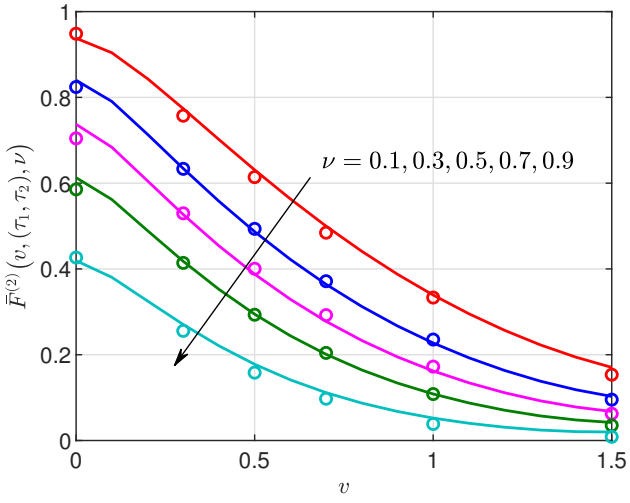

(c) $\tau_1 = \tau_2 = 0$ dB

Fig. 7. Product MD of SIR with different τ_1, τ_2 and reliabilities ν for 1D Poisson networks. The lines show the analytical results approximated by the beta distribution and the moments in Theorem 1. The markers are the simulation results.

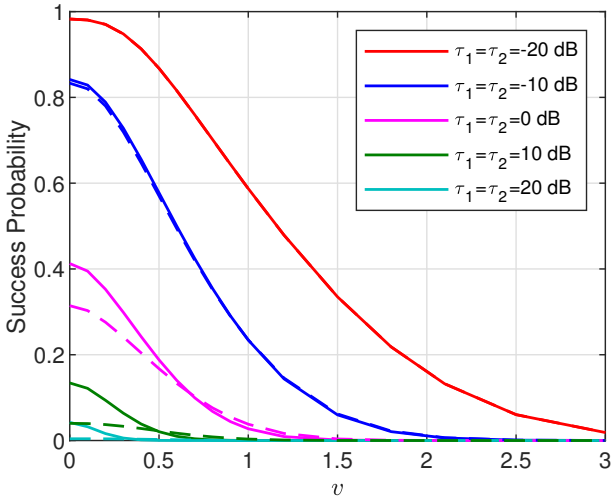

(a) Joint Success Probability $M_1^{(2)}$

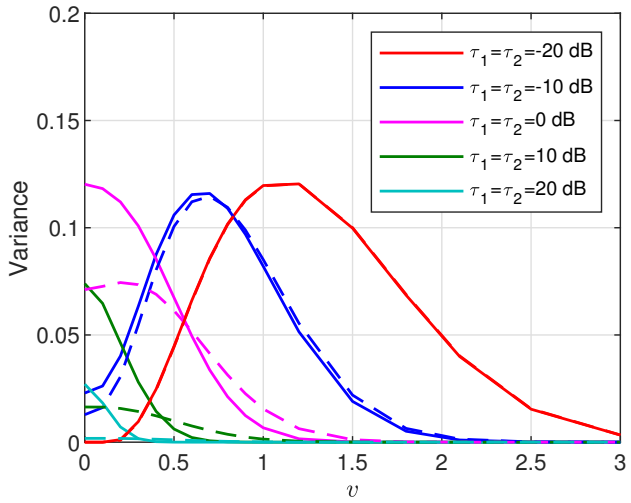

(b) Variance $M_2^{(2)} - (M_1^{(2)})^2$

Fig. 8. The success probability $M_1^{(2)}$ and the variance $M_2^{(2)} - (M_1^{(2)})^2$ for 2D Poisson networks. The dashed lines are obtained under the independent SIRs assumption from Remark 1.

moments (6), as the analytical approximation to the MD. As will be observed from the comparison with simulation results, the approximation is very accurate also for the product MD.

For the 1D Poisson network model, Fig. 6 shows the success probability and variance, and Fig. 7 shows the MD of SIR as a function of v for different τ_1, τ_2. The solid lines are from Theorem 1. For the 2D Poisson network model, Fig. 8 shows the success probability and variance, and Fig. 9 shows the SIR MD. In these figures, the solid lines are from Theorem 2, the dashed lines are under the independent SIRs assumption from Remark 1. By comparing the results from Theorem 2 and Remark 1, we can find that the dependence of the SIRs for UE1 and UE2 cannot be ignored for larger SIR thresholds τ_1, τ_2. On the other hand, for small thresholds, the assumption of independent SIRs has only a small effect.

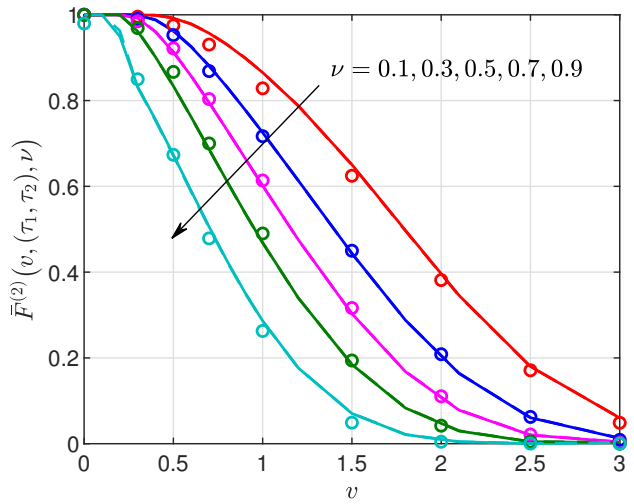

(a) $\tau_1 = \tau_2 = -20$ dB

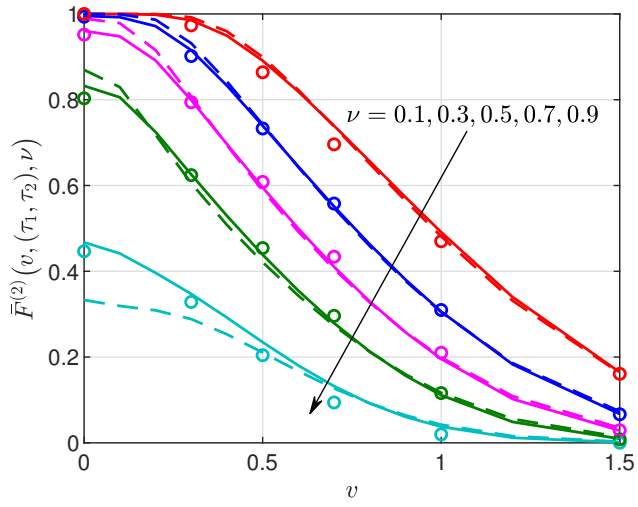

(b) $\tau_1 = \tau_2 = -10$ dB

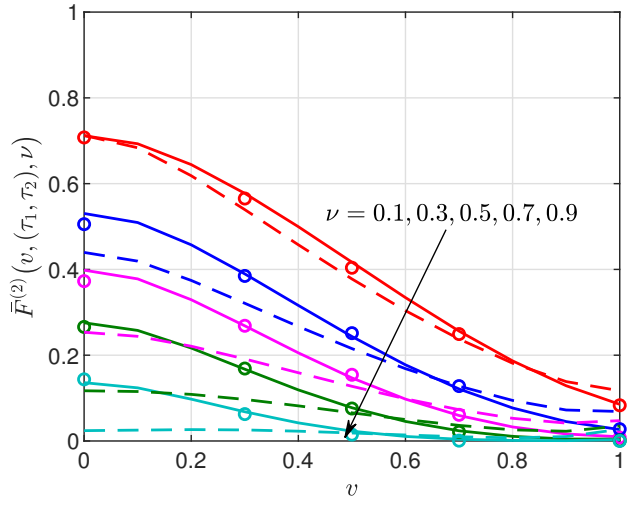

(c) $\tau_1 = \tau_2 = 0$ dB

Fig. 9. Product MD with different τ_1, τ_2 and reliabilities ν for 2D Poisson networks. The markers are the simulation results. The dashed lines are obtained under the independent SIRs assumption from Remark 1.

IV. Application to Physical Layer Security

In this section, we apply the 2D Poisson network model in Sec. III-A and the product MD to physical layer security in a downlink cellular network. We set UE1 as the typical legitimate user. We focus on passive eavesdropping, where an eavesdropper intercepts the signal without any attack. The eavesdropper is assumed to be located at $(v,0)$, i.e., UE2 in the 2D Poisson network model. Then, the SIR of the legitimate user (UE1) is given in (14), while the received SIR of the eavesdropper (UE2) is given in (15).

The event of opportunistic secure spectrum access (OSSA) defined in [18] is that the eavesdropper cannot decode the message from the BS (secrecy success) while the legitimate user can (connection success). Following the definition of the OSSA probability, we next define the *conditional* OSSA probability and its MD.

A. Conditional OSSA Probability and its Meta Distribution

We define the following three success probabilities for the confidential message transmission.

- **Conditional connection success probability**: The probability that the SIR from the serving BS to the legitimate user (UE1) is above the threshold τ_1 given the point process Φ, denoted by $P_{\rm cs}(\tau_1)=\mathbb{P}(\mathrm{SIR}_1>\tau_1 \mid \Phi)$.
- **Conditional secrecy success probability**: The probability that the SIR from the typical user's serving BS to the eavesdropper (UE2) is below the threshold τ_2 given the point process Φ, denoted by $P_{\rm ss}(\tau_2)=\mathbb{P}(\mathrm{SIR}_2<\tau_2 \mid \Phi)$.
- **Conditional OSSA probability**: The probability of OSSA given the point process Φ, denoted by $P_{\rm OSSA}$, i.e., the conditional probability of the event of both connection success and secrecy success. Due to the conditional independence given Φ, $P_{\rm OSSA}=P_{\rm cs}(\tau_1)P_{\rm ss}(\tau_2)$.

Then, the MD of the conditional OSSA probability can be defined as

$$\begin{aligned}\bar{F}_{\rm OSSA}(\nu) &\triangleq \mathbb{P}(P_{\rm OSSA}>\nu)\\ &=\mathbb{P}(\mathbb{P}(\mathrm{SIR}_1>\tau_1 \mid \Phi)\mathbb{P}(\mathrm{SIR}_2<\tau_2 \mid \Phi)>\nu).\end{aligned} \tag{34}$$

B. Moments of the Conditional OSSA Probability

Theorem 3 (The b-th moment of $P_{\rm OSSA}$) *The b-th moment $M_b^{\rm OSSA}(v)$ of the conditional OSSA probability $P_{\rm OSSA}$ is*

$$\begin{aligned}M_b^{\rm OSSA}(v)=\sum_{k=0}^{\infty}\binom{b}{k}(-1)^k\int_0^{2\pi}\int_0^{\infty}\frac{f_{R_1}(r)}{2\pi}\\ \cdot\exp\Big(-\int_0^{2\pi}\int_r^{\infty}G_{b,k}\ \lambda z\mathrm{d}z\mathrm{d}\omega\Big)\mathrm{d}r\mathrm{d}\theta,\ b\in\mathbb{C},\end{aligned} \tag{35}$$

where $f_{R_1}(r)$ is given by (21)*, and*

$$G_{b,k}=1-\frac{\left(1+\tau_1 r^{\alpha}z^{-\alpha}\right)^{-b}}{\left(1+\tau_2\left(\frac{r^2+v^2-2rv\cos\theta}{z^2+v^2-2zv\cos\omega}\right)^{\frac{\alpha}{2}}\right)^k}. \tag{36}$$

Proof: The conditional connection success probability for the legitimate user (UE1) is given by (see (16))

$$P_{\rm cs}(\tau_1)=\prod_{z\in\Phi\setminus\{s(o)\}}\frac{1}{1+\frac{\tau_1 R_1^{\alpha}}{\|z\|^{\alpha}}}, \tag{37}$$

and the conditional secrecy success probability for the eavesdropper (UE2) is given by

$$P_{\rm ss}(\tau_2)=1-\prod_{z\in\Phi\setminus\{s(o)\}}\frac{1}{1+\frac{\tau_2\|(v,0)-s(o)\|^{\alpha}}{\|(v,0)-z\|^{\alpha}}}. \tag{38}$$

The b-th moment of the conditional OSSA probability can be obtained as

$$\begin{aligned}M_b^{\rm OSSA}(v)&=\mathbb{E}(P_{\rm OSSA}^b)=\mathbb{E}(P_{\rm cs}^b(\tau_1)P_{\rm ss}^b(\tau_2))\\ &=\mathbb{E}(P_{\rm cs}^b(\tau_1)(1-\bar{P}_{\rm ss}(\tau_2))^b)\\ &=\sum_{k=0}^{\infty}\binom{b}{k}(-1)^k\underbrace{\mathbb{E}(P_{\rm cs}^b(\tau_1)\bar{P}_{\rm ss}^k(\tau_2))}_{M_{b,k}}.\end{aligned} \tag{39}$$

The term $M_{b,k}$ in (39) can be expressed by a direct extension of Theorem 2 as

$$\begin{aligned}M_{b,k}&=\mathbb{E}\Bigg(\prod_{z\in\Phi\setminus\{s(o)\}}\left(\frac{1}{1+\frac{\tau_1 R_1^{\alpha}}{\|z\|^{\alpha}}}\right)^b\left(\frac{1}{1+\frac{\tau_2\|(v,0)-s(o)\|^{\alpha}}{\|(v,0)-z\|^{\alpha}}}\right)^k\Bigg)\\ &=\int_0^{2\pi}\int_0^{\infty}\exp\Big(-\int_0^{2\pi}\int_r^{\infty}G_{b,k}\lambda z\mathrm{d}z\mathrm{d}\omega\Big)\frac{f_{R_1}(r)}{2\pi}\mathrm{d}r\mathrm{d}\theta,\end{aligned} \tag{40}$$

where $f_{R_1}(r)$ is given by (21), and $G_{b,k}$ is given by (36). Substituting the result of (39), the result follows. ∎

Remark 2: It is easy to obtain $M_1^{\rm OSSA}(v)$ (the OSSA probability) and $M_2^{\rm OSSA}(v)$ from Theorem 3. The first moment $M_1^{\rm OSSA}(v)$ of the conditional OSSA probability $P_{\rm OSSA}$ is

$$\begin{aligned}M_1^{\rm OSSA}(v)&=\frac{1}{{}_2F_1(1,-\delta;1-\delta;-\tau_1)}\\ &-\int_0^{2\pi}\int_0^{\infty}\exp\Big(-\lambda\int_0^{2\pi}\int_r^{\infty}G_{1,1}z\mathrm{d}z\mathrm{d}\omega\Big)\frac{f_{R_1}(r)}{2\pi}\mathrm{d}r\mathrm{d}\theta,\end{aligned} \tag{41}$$

which is the same as [18, Thm. 1] when the jamming is eliminated, and the second moment $M_2^{\rm OSSA}(v)$ of the conditional OSSA probability $P_{\rm OSSA}$ is

$$\begin{aligned}M_2^{\rm OSSA}(v)&=\frac{1}{{}_2F_1\left(2,-\delta;1-\delta;-\tau_1\right)}\\ &-2\int_0^{2\pi}\int_0^{\infty}\exp\Big(-\lambda\int_0^{2\pi}\int_r^{\infty}G_{2,1}z\mathrm{d}z\mathrm{d}\omega\Big)\frac{f_{R_1}(r)}{2\pi}\mathrm{d}r\mathrm{d}\theta\\ &+\int_0^{2\pi}\int_0^{\infty}\exp\Big(-\lambda\int_0^{2\pi}\int_r^{\infty}G_{2,2}z\mathrm{d}z\mathrm{d}\omega\Big)\frac{f_{R_1}(r)}{2\pi}\mathrm{d}r\mathrm{d}\theta,\end{aligned} \tag{42}$$

where $\delta=2/\alpha$. Generally, if b is a positive integer, the infinite sum in (35) reduces to a finite sum from 0 to b.

Remark 3 (The b-th moment for independent SIRs): If the SIRs are assumed independent for the legitimate user (UE1) and its eavesdropper (UE2), the b-th moment is given by

$$\begin{aligned}\tilde{M}_b^{\rm OSSA}(v)&=\mathbb{E}(\mathbb{P}(\mathrm{SIR}_1>\tau_1 \mid \Phi)^b)\mathbb{E}(\mathbb{P}(\mathrm{SIR}_2<\tau_2 \mid \Phi)^b)\\ &=\frac{1}{{}_2F_1(b,-\delta;1-\delta;-\tau_1)}M_{b2},\end{aligned} \tag{43}$$

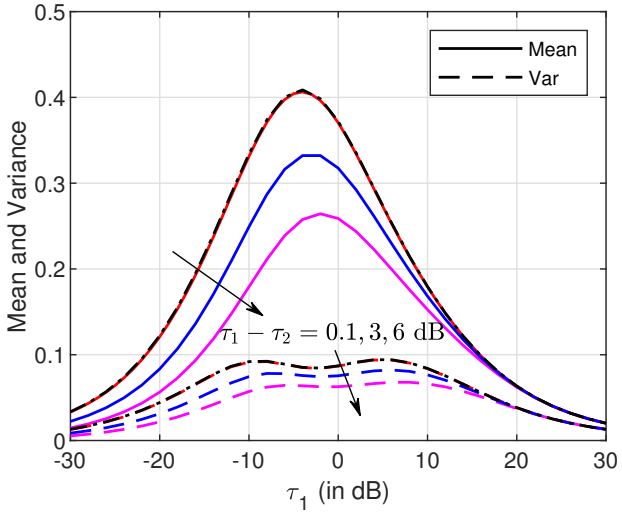

Fig. 10. The mean (success probability) $M_1^{\mathrm{OSSA}}(v)$ and the variance $M_2^{\mathrm{OSSA}}(v) - (M_1^{\mathrm{OSSA}}(v))^2$ of P_{OSSA} with $\tau_1 - \tau_2 = \{0.1, 3, 6\}$ dB, $v = \frac{1}{2\sqrt{\lambda}}$, and $\alpha = 4$. The solid lines show the OSSA probability, and the dashed lines show the variance of P_{OSSA}. The dash-dotted lines are the results for $\tau_1 = \tau_2$, which is the boundary of the region of secure communication.

where

$$M_{b2} = \sum_{k=0}^{\infty} \binom{b}{k} (-1)^k \int_0^{2\pi} \int_0^{\infty} \frac{f_{R_1}(r)}{2\pi} \cdot \exp\left(- \int_0^{2\pi} \int_r^{\infty} G_{0,k} \lambda z \mathrm{d}z \mathrm{d}\omega \right) \mathrm{d}r \mathrm{d}\theta, \quad (44)$$

$$G_{0,k} = 1 - \left(1 + \tau_2 \left(\frac{r^2 + v^2 - 2rv\cos\theta}{z^2 + v^2 - 2zv\cos\omega} \right)^{\frac{\alpha}{2}} \right)^{-k} \quad (45)$$

is the b-th moment for the eavesdropper (UE2).

Remark 4 (Asymptotic behavior as $\tau_2 \to \infty$ or $v \to \infty$): When $\tau_2 \to \infty$ or $v \to \infty$, we both have $\mathbb{P}\left(\mathrm{SIR}_2 < \tau_2 \mid \Phi\right) \to 1$, hence

$$M_b^{\mathrm{OSSA}}(v) = \mathbb{E}(\mathbb{P}(\mathrm{SIR}_1 > \tau_1 \mid \Phi)^b \mathbb{P}(\mathrm{SIR}_2 < \tau_2 \mid \Phi)^b) = \frac{1}{{}_2F_1\left(b, -\delta; 1-\delta; -\tau_1\right)}, \quad (46)$$

i.e., $M_b^{\mathrm{OSSA}}(v)$ approaches the standard b-th moment without secrecy constraint, as shown in Fig. 14 and Fig. 15.

C. Numerical Results

The intensity of the BSs used in this section is $\lambda = 1$. We set $v = \frac{1}{2\sqrt{\lambda}} = \frac{1}{2}$ in most figures in this section, which is the average distance between a BS and its nearest neighbor. The same value is used in [18]. According to Wyner's encoding scheme [27], $\mathrm{SIR}_1 > \mathrm{SIR}_2$ is needed to communicate securely, i.e., $\tau_1 > \tau_2$. Hence, we set $\tau_1 - \tau_2 = 0.1$ (all in dB) for most of the results about the OSSA probability, the variance and the MD, and in Figs. 13–15 we use various values of α, τ_2 and v for comparison.

Fig. 10 shows the OSSA probability and variance with $\tau_1 - \tau_2 = 0.1, 3, 6$ dB, and the results for $\tau_1 = \tau_2$, which is the boundary of the region of secure communication. Fig. 11 shows the OSSA probability (mean) and variance against τ_1 (and τ_2) for the actual network (where the SIRs are correlated) and under the assumption of independent SIRs. It is apparent that the SIRs correlation leads to a decrease in the OSSA probability and variance. Fig. 12 shows the MD of the conditional OSSA probability, which is approximated by the beta distribution and the simulation in the Poisson cellular network. The MD shows the proportion of the links with both connection and secrecy success given a target reliability. For the chosen parameters, with the increase of the required reliability, the number of these links is gradually decreasing with decreasing speed as ν approaches 1. Fig. 13(a) shows that with the increase of α, the OSSA probability and the variance increase, and the peak of the OSSA probability will shift to the right, while the variance stays basically the same. Fig. 13(b) indicates that as α decreases, the MD decreases for

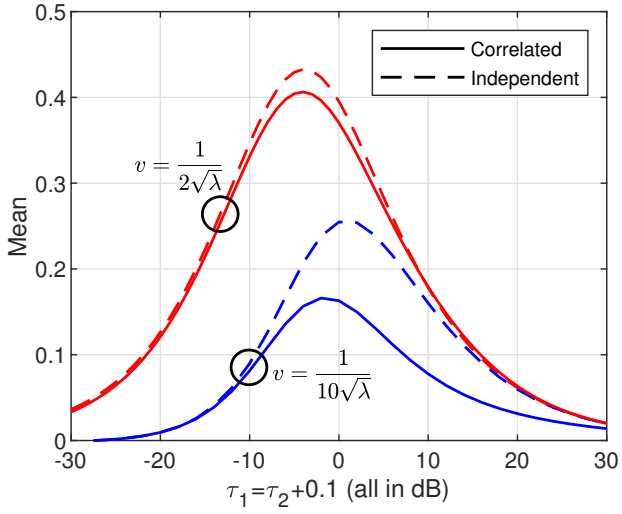

(a) Mean $M_1^{\mathrm{OSSA}}(v)$

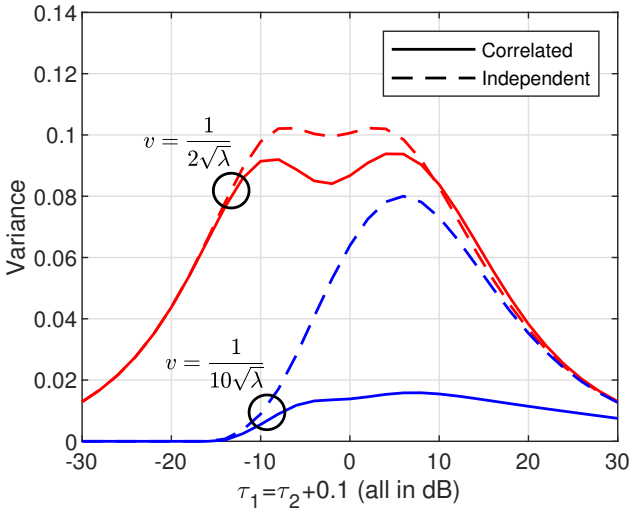

(b) Variance $M_2^{\mathrm{OSSA}}(v) - (M_1^{\mathrm{OSSA}}(v))^2$

Fig. 11. The mean (success probability) and the variance of P_{OSSA} at $\alpha = 4$ for the network. The solid lines show the OSSA probability and variance when the SIRs are correlated (i.e., Theorem 3). The dashed lines show the OSSA probability and variance when the SIRs are assumed independent (i.e., Remark 3).

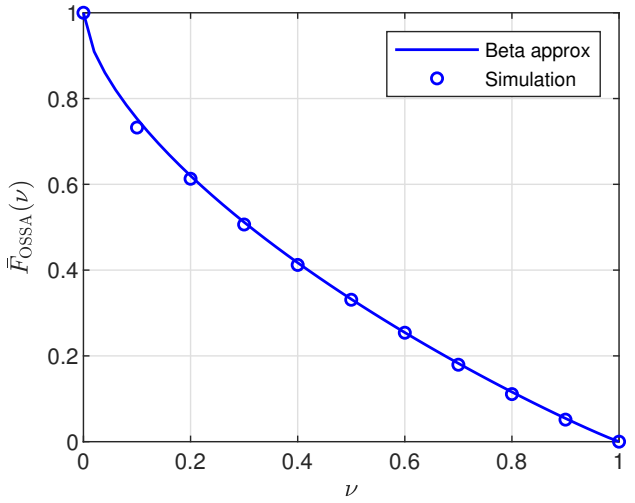

Fig. 12. The MD at $\tau_1 = 0$ dB, $\tau_2 = -0.1$ dB, $v = \frac{1}{2\sqrt{\lambda}}$ and $\alpha = 4$. The solid line shows the MD approximated by the beta distribution. Markers show the results of the Monte Carlo simulations.

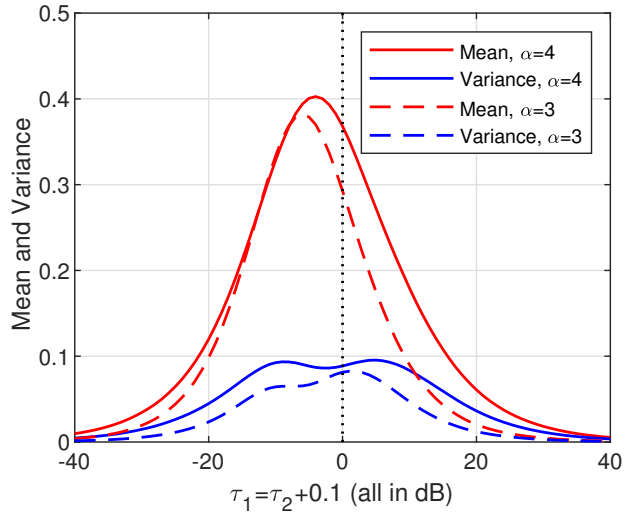

(a) Mean $M_1^{\mathrm{OSSA}}(v)$ and Variance $M_2^{\mathrm{OSSA}}(v) - (M_1^{\mathrm{OSSA}}(v))^2$

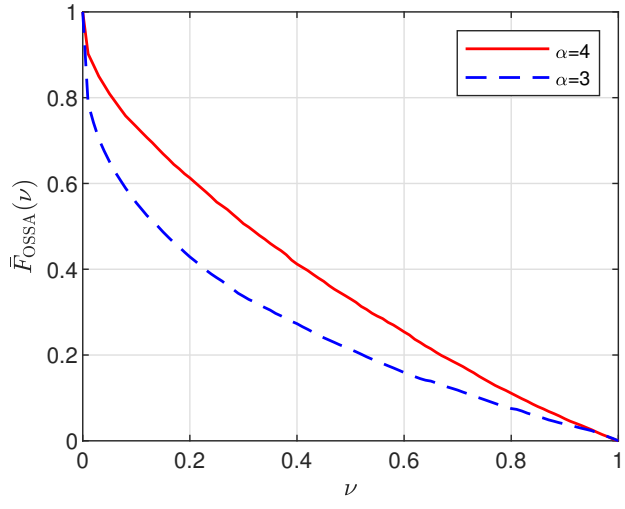

(b) MD ($\tau_1 = 0$ dB, $\tau_2 = -0.1$ dB)

Fig. 13. The mean, the variance, and the MD at $v = \frac{1}{2\sqrt{\lambda}}$. The dashed lines and the solid lines show the results with $\alpha = 3, 4$ respectively.

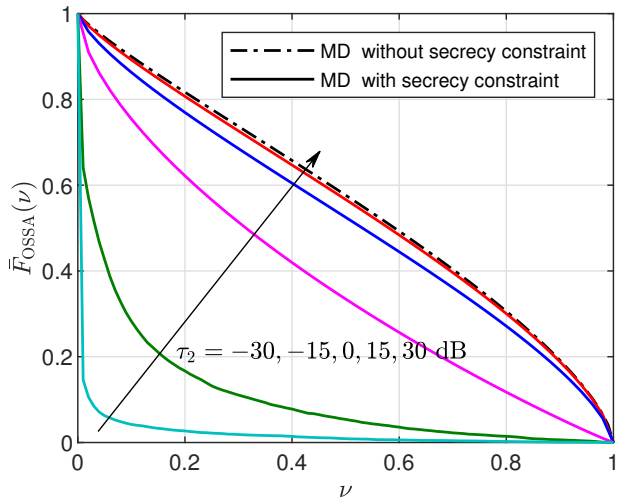

Fig. 14. The MD at $\tau_1 = 0$ dB, $\alpha = 4$ and $v = \frac{1}{2\sqrt{\lambda}}$. The dash-dotted line shows the standard MD without secrecy constraint (i.e., Remark 4), and the solid lines show the MD with secrecy constraint (i.e., Theorem 3) when $\tau_2 = -30, -15, 0, 15, 30$ dB.

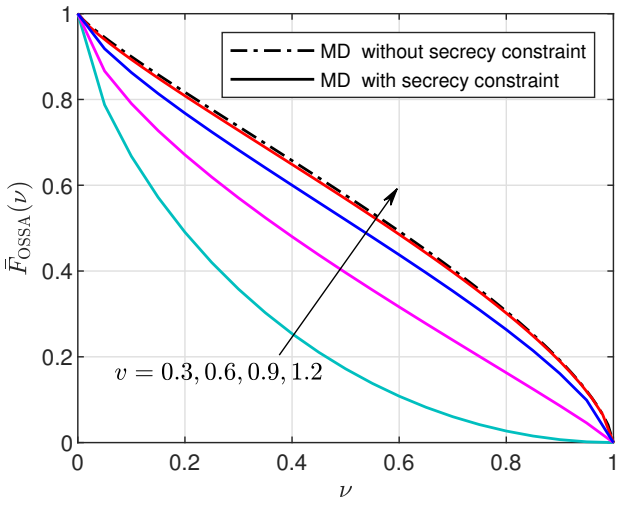

Fig. 15. The MD at $\tau_1 = 0$ dB, $\tau_2 = -0.1$ dB and $\alpha = 4$. The dash-dotted line shows the standard MD, and the solid lines show the MD with secrecy constrain when $v = 0.3, 0.6, 0.9, 1.2$. The MD at $v = \frac{1}{2\sqrt{\lambda}} = 0.5$ is shown in Fig. 12.

all $\nu \in [0, 1]$, and it decreases faster when ν is smaller. Fig. 14 shows when $\tau_1 = 0$ dB and τ_2 varies, where a smaller τ_2 means a higher security level, the link reliability of the network will decrease. And as the secrecy constraint decreases, i.e., τ_2 increases, the curves will approach the standard MD quickly. Fig. 15 shows that when the eavesdropper is far away from the typical user relative to the distance from the user to its serving BS, the link reliability of the network will also increase and approach to the MD without secrecy constraint gradually. Fig. 16 shows the impact of the distance v on the OSSA probability, the variance of conditional OSSA probability, and its MD. The results of the the OSSA probability are consistent with [18], although the setup of λ and v is different. As the distance v increases, the correlation of legitimate user and its eavesdropper decreases. Hence, the error caused by the

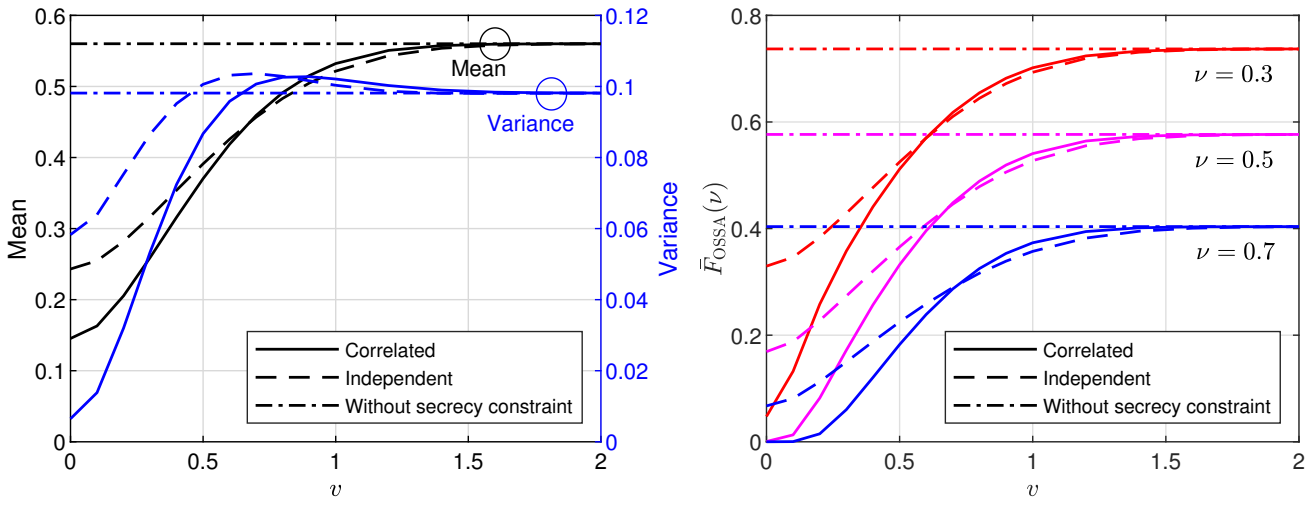

(a) Mean $M_1^{\mathrm{OSSA}}(v)$ and Variance $M_2^{\mathrm{OSSA}}(v) - (M_1^{\mathrm{OSSA}}(v))^2$

(b) MD

Fig. 16. The mean, the variance, and the MD at $\tau_1 = 0$ dB, $\tau_2 = -0.1$ dB. The solid lines show the results when the SIRs are correlated (i.e., Theorem 3), and the dashed lines show the results when the SIRs are assumed independent (i.e., Remark 3). The dash-dotted lines show the results without secrecy constraint (i.e., Remark 4).

independence assumption of SIRs is decreasing. Besides, the results with secrecy constraint are approaching the standard single-user results including success probability, variance, and MD.

V. Application to Cooperative Reception

Here we consider the scenario where the BS sends a message to a group of users, and the goal is that at least one user successfully receives the message. We again use the 2D Poisson network model in Sec. III-A. Two users, UE1 located at the origin and UE2 located at $(v, 0)$, attempt to receive the message from UE1's serving BS as a group. The received SIRs of UE1 and UE2 are given by (14) and (15).

A. The SIR Meta Distribution

According to this system model and letting $\tau = \tau_1 = \tau_2$, due to the conditional independence of the SIR_i given Φ, the joint conditional outage probability $\bar{P}_{\mathrm{CR}} = 1 - P_{\mathrm{CR}}$ can be expressed as

$$\begin{aligned}\bar{P}_{\mathrm{CR}} &= \mathbb{P}(\mathrm{SIR}_1 < \tau \mid \Phi)\mathbb{P}(\mathrm{SIR}_2 < \tau \mid \Phi) \\ &= 1 - P_1(\tau) - P_2(\tau) + P_1(\tau)P_2(\tau), \end{aligned} \tag{47}$$

where P_{CR} is the conditional probability for the event that the transmission succeeds at any one of the two users, or both. The MD of P_{CR} follows as

$$\begin{aligned}\bar{F}_{\mathrm{CR}}(\nu) &= \mathbb{P}(P_{\mathrm{CR}} > \nu) \\ &= \mathbb{P}(1 - \mathbb{P}(\mathrm{SIR}_1 < \tau \mid \Phi)\mathbb{P}(\mathrm{SIR}_2 < \tau \mid \Phi) > \nu). \end{aligned} \tag{48}$$

Theorem 4 (First and second moments of P_{CR}) *The first and second moments of P_{CR} can be expressed as*

$$M_1^{\mathrm{CR}}(v) = M_{1,0} + M_{0,1} - M_{1,1}, \tag{49}$$

$$M_2^{\mathrm{CR}}(v) = M_{2,0} + M_{0,2} + 2M_{1,1} - 2M_{2,1} - 2M_{1,2} + M_{2,2}, \tag{50}$$

where

$$M_{i,j} = \int_0^{2\pi}\int_0^{\infty} \frac{f_{R_1}(r)}{2\pi} \exp\Bigg(- \int_0^{2\pi}\int_r^{\infty} \lambda z \cdot \left(1 - \frac{\left(1 + \tau r^{\alpha} z^{-\alpha}\right)^{-i}}{\left(1 + \tau\left(\frac{r^2+v^2-2rv\cos\theta}{z^2+v^2-2zv\cos\omega}\right)^{\frac{\alpha}{2}}\right)^{j}}\right) \mathrm{d}z\mathrm{d}\omega \Bigg) \mathrm{d}r\mathrm{d}\theta, \tag{51}$$

and $f_{R_1}(r)$ is given by (21).

Proof: The b-th moment $M_b^{\mathrm{CR}}(v)$ of P_{CR} is

$$M_b^{\mathrm{CR}}(v) \triangleq \mathbb{E}((P_1(\tau) + P_2(\tau) - P_1(\tau)P_2(\tau))^b). \tag{52}$$

For $b = 1$ and $b = 2$, letting $M_{i,j} = \mathbb{E}(P_1^i(\tau)P_2^j(\tau))$, (49) and (50) are obtained from (52), and $M_{i,j}$ can be given by (40). ∎

Remark 5: For $v = 0$, the moments can be simplified to

$$M_1^{\mathrm{CR}}(0) = M_{1,0} + M_{0,1} - M_{1,1}, \tag{53}$$

$$M_2^{\mathrm{CR}}(0) = M_{2,0} + M_{0,2} + 2M_{1,1} - 2M_{2,1} - 2M_{1,2} + M_{2,2}, \tag{54}$$

where

$$\begin{aligned} M_{i,j} &= \int_0^{\infty} \exp\left(-\int_r^{\infty}\left(1 - \frac{1}{\left(1 + \tau\frac{r^{\alpha}}{z^{\alpha}}\right)^{i+j}}\right) 2\pi\lambda z \mathrm{d}z\right) f_{R_1}(r)\mathrm{d}r \\ &= \int_0^{\infty} \exp\left(-\pi\lambda r^2\left(-1 + {}_2F_1\left(i+j, -\delta; 1-\delta; -\tau\right)\right)\right) f_{R_1}(r)\mathrm{d}r \\ &= \frac{1}{{}_2F_1\left(i+j, -\delta; 1-\delta; -\tau\right)}. \end{aligned} \tag{55}$$

These moments correspond to those for Type-I HARQ with 2 (re)transmissions [28, Thm. 1], since the system models of these two scenarios are essentially the same.

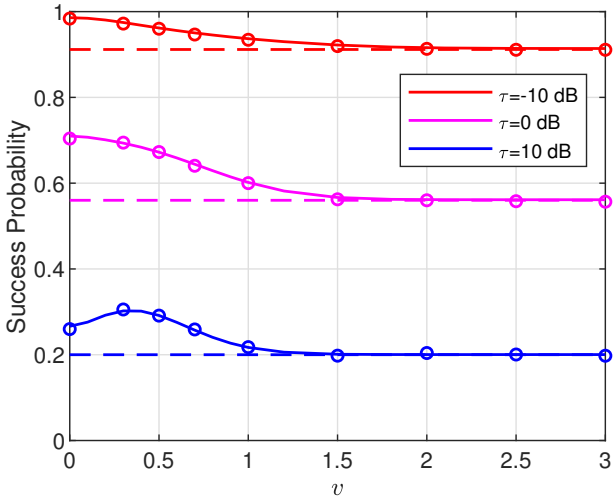

(a) Joint Success Probability $M_1^{\mathrm{CR}}(v)$

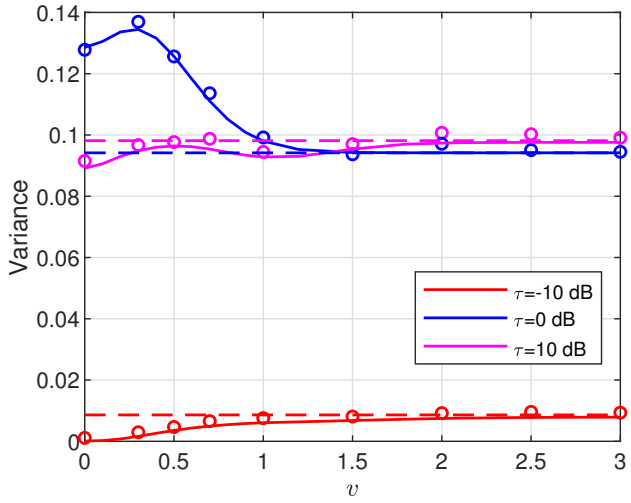

(b) Variance $M_2^{\mathrm{CR}}(v) - (M_1^{\mathrm{CR}}(v))^2$

Fig. 17. The success probability $M_1^{\mathrm{CR}}(v)$ and the variance $M_2^{\mathrm{CR}}(v) - (M_1^{\mathrm{CR}}(v))^2$ for 2D Poisson networks with cooperative reception. The dashed lines shows the success probabilities and variances at UE1 only, i.e., the results without cooperative reception.

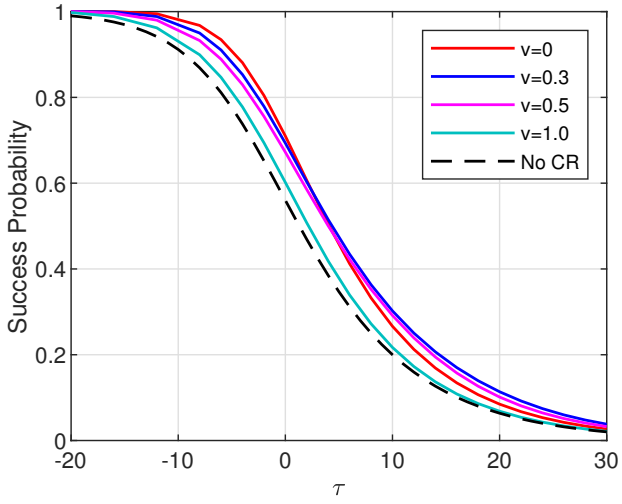

(a) Joint Success Probability $M_1^{\mathrm{CR}}(v)$

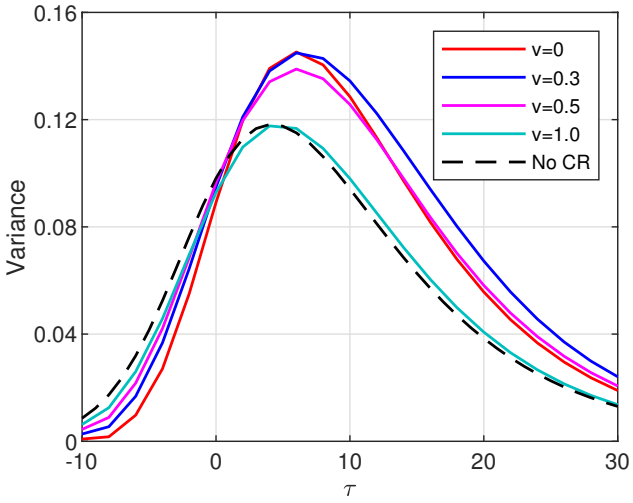

(b) Variance $M_2^{\mathrm{CR}}(v) - (M_1^{\mathrm{CR}}(v))^2$

Fig. 18. The success probability $M_1^{\mathrm{CR}}(v)$ and the variance $M_2^{\mathrm{CR}}(v) - (M_1^{\mathrm{CR}}(v))^2$ for 2D Poisson networks with cooperative reception. Markers show the results of the Monte Carlo simulations. The dashed lines show the results without cooperative reception.

B. Numerical Results

Here we show the numerical results and some simulation results. The intensity of the BSs used in this section is $\lambda = 1$. The path loss exponent is $\alpha = 4$. Again $v = \frac{1}{2\sqrt{\lambda}} = 0.5$. Fig. 17 and Fig. 18 show the success probability and variance with different v and τ. The dashed lines in Fig. 17 and 18 are the results without cooperative reception, i.e., only UE1 is considered. Fig. 19 and Fig. 20 shows the MD of SIR with different threshold τ, reliability ν, and distance v. We can see from this figure that the SIR performance benefit of cooperative reception is decreasing as the distance v between UE1 and UE2 increases. For $v > 1$, there is little benefit in cooperative reception.

VI. Conclusions

In this paper, the joint MD of the SIR is formally defined for multiple users, as well as the joint conditional success probability and n-th order product MD. We find that the dependence of the SIRs for UE1 and UE2 cannot be ignored for larger SIR thresholds τ_1, τ_2. The distribution of the distances of UE1 and UE2 to their closest interferer and serving BS shows that the distance of UE2 to its serving BS becomes the main factor affecting the SIR for larger distance v between the users.

The joint MD is applied to physical layer security and cooperative reception. For the application to physical layer security, we find that when the eavesdropper is far away from the legitimate user relative to the distance from the user to its serving BS, the link reliability of the network will also increase and approach the MD without secrecy constraint gradually. And given the threshold of connection success, a smaller threshold of secrecy success means a higher security level, and the link reliability of the network will decrease. As the secrecy constraint decreases, i.e., the threshold of secrecy

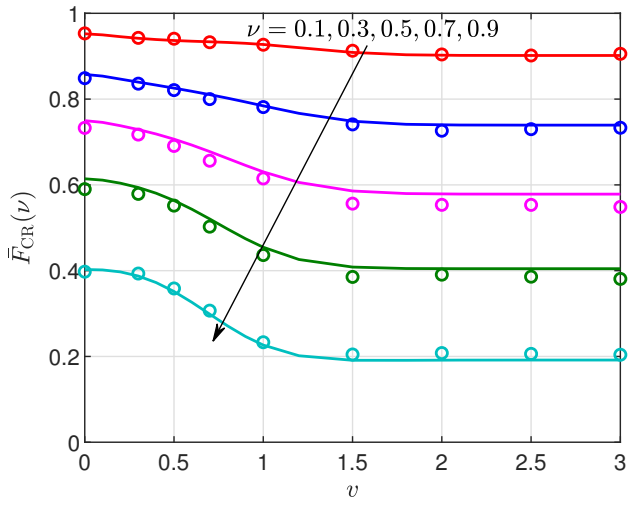

(a) $\tau = 0$ dB

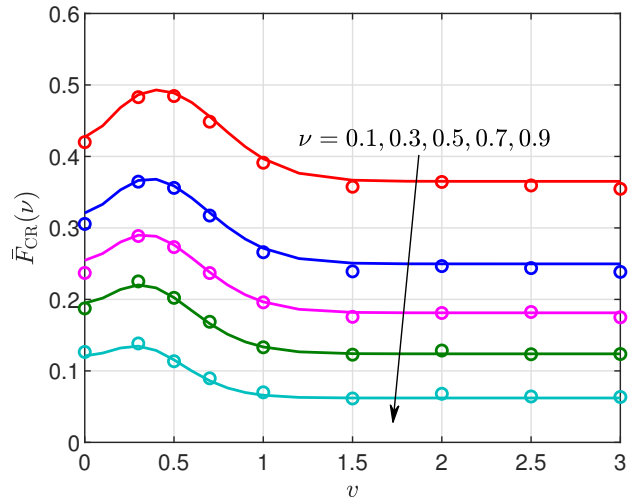

(b) $\tau = 10$ dB

Fig. 19. The MD of SIRs as a function of v for different reliabilities ν for 2D Poisson networks with cooperative reception. The lines show the analytical results approximated by the beta distribution. Markers show the results of the Monte Carlo simulations.

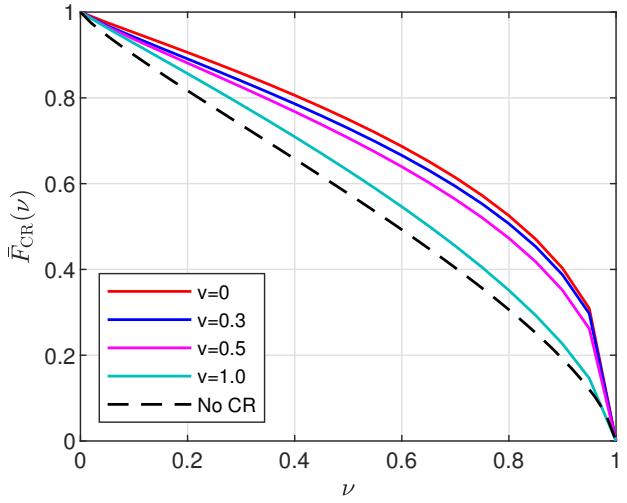

Fig. 20. The MD of SIRs for $\tau = 0$ dB, and different distances v for 2D Poisson networks with cooperative reception. The dashed line shows the result without cooperative reception.

success increases, the curves will approach the standard MD quickly. For the application to cooperative reception, the SIR performance benefit of cooperative reception is decreasing as the distance v between UE1 and UE2 increases. At a large v, there is little benefit in cooperative reception.

Overall, the concept of the joint MD permits a refined performance analysis of wireless networks when multiple links are involved.

References

[1] Q. Cui, X. Jiang, X. Yu, Y. Wang, and M. Haenggi, "SIR meta distribution in physical layer security with interference correlation," in *Proceedings of 2018 IEEE Global Communications Conference (GLOBECOM'18)*, Abu Dhabi, UAE, Dec. 2018.

[2] M. Agiwal, A. Roy, and N. Saxena, "Next generation 5G wireless networks: A comprehensive survey," *IEEE Commun. Surveys Tuts.*, vol. 18, no. 3, pp. 1617–1655, thirdquarter 2016.

[3] B. Błaszczyszyn, M. Haenggi, P. Keeler, and S. Mukherjee, *Stochastic geometry analysis of cellular networks*. Cambridge, United Kingdom; New York, NY, USA: Cambridge University Press, 2018.

[4] J. G. Andrews, F. Baccelli, and R. K. Ganti, "A tractable approach to coverage and rate in cellular networks," *IEEE Trans. Commun.*, vol. 59, no. 11, pp. 3122–3134, Nov. 2011.

[5] H. ElSawy, E. Hossain, and M. Haenggi, "Stochastic geometry for modeling, analysis, and design of multi-tier and cognitive cellular wireless networks: A survey," *IEEE Commun. Surveys Tuts.*, vol. 15, no. 3, pp. 996–1019, thirdquarter 2013.

[6] M. Haenggi, "The meta distribution of the SIR in Poisson bipolar and cellular networks," *IEEE Trans. Wireless Commun.*, vol. 15, no. 4, pp. 2577–2589, Apr. 2016.

[7] M. Salehi, A. Mohammadi, and M. Haenggi, "Analysis of D2D underlaid cellular networks: SIR meta distribution and mean local delay," *IEEE Trans. Commun.*, vol. 65, no. 7, pp. 2904–2916, Jul. 2017.

[8] N. Deng and M. Haenggi, "A fine-grained analysis of millimeter-wave device-to-device networks," *IEEE Trans. Commun.*, vol. 65, no. 11, pp. 4940–4954, Nov. 2017.

[9] Q. Cui, X. Yu, Y. Wang, and M. Haenggi, "The SIR meta distribution in Poisson cellular networks with base station cooperation," *IEEE Trans. Commun.*, vol. 66, no. 3, pp. 1234–1249, Mar. 2018.

[10] J. Tang, G. Chen, and J. P. Coon, "The meta distribution of the secrecy rate in the presence of randomly located eavesdroppers," *IEEE Wireless Commun. Lett.*, vol. 7, no. 4, pp. 630–633, Aug. 2018.

[11] S. Krishnan and H. S. Dhillon, "Spatio-temporal interference correlation and joint coverage in cellular networks," *IEEE Trans. Wireless Commun.*, vol. 16, no. 9, pp. 5659–5672, Sep. 2017.

[12] S. Sadr and R. S. Adve, "Handoff rate and coverage analysis in multi-tier heterogeneous networks," *IEEE Trans. Wireless Commun.*, vol. 14, no. 5, pp. 2626–2638, May 2015.

[13] J. Tang, G. Chen, and J. P. Coon, "Joint coverage enhancement by power allocation in Poisson clustered out-of-band D2D networks," *IEEE Trans. Veh. Technol.*, vol. 67, no. 12, pp. 11 537–11 548, Dec. 2018.

[14] S. Singh, X. Zhang, and J. G. Andrews, "Joint rate and SINR coverage analysis for decoupled uplink-downlink biased cell associations in HetNets," *IEEE Trans. Wireless Commun.*, vol. 14, no. 10, pp. 5360–5373, Oct. 2015.

[15] M. A. Kishk and H. S. Dhillon, "Joint uplink and downlink coverage analysis of cellular-based RF-powered IoT network," *IEEE Transactions on Green Communications and Networking*, vol. 2, no. 2, pp. 446–459, Jun. 2017.

[16] R. Tanbourgi, H. S. Dhillon, and F. K. Jondral, "Analysis of joint transmit–receive diversity in downlink MIMO heterogeneous cellular networks," *IEEE Trans. Wireless Commun.*, vol. 14, no. 12, pp. 6695–6709, Dec. 2015.

[17] J. Wen, M. Sheng, K. Huang, and J. Li, "Effects of base-station spatial interdependence on interference correlation and network performance," *IEEE Trans. Commun.*, vol. 66, no. 7, pp. 3092–3107, Jul. 2018.

[18] K. S. Ali, H. ElSawy, M. Haenggi, and M.-S. Alouini, "The effect of spatial interference correlation and jamming on secrecy in cellular networks," *IEEE Wireless Commun. Lett.*, vol. 6, no. 4, pp. 530–533, Aug. 2017.

[19] M. Haenggi, "Efficient calculation of meta distributions and the performance of user percentiles," *IEEE Wireless Commun. Lett.*, vol. 7, no. 6, pp. 982–985, Dec. 2018.

[20] ——, *Stochastic Geometry for Wireless Networks*. New York, USA: Cambridge University Press, 2012.
[21] V. V. Chetlur and H. S. Dhillon, "Coverage analysis of a vehicular network modeled as Cox process driven by Poisson line process," *IEEE Trans. Wireless Commun.*, vol. 17, no. 7, pp. 4401–4416, Jul. 2018.
[22] M. Sikora, J. N. Laneman, M. Haenggi, D. J. Costello, and T. E. Fuja, "Bandwidth- and power-efficient routing in linear wireless networks," *Joint Special Issue of IEEE Trans. Inf. Theory and IEEE/ACM Trans. Netw.*, vol. 52, no. 6, pp. 2624–2633, Jun. 2006.
[23] B. Błaszczyszyn and P. Mühlethaler, "Random linear multihop relaying in a general field of interferers using spatial Aloha," *IEEE Trans. Wireless Commun.*, vol. 14, no. 7, pp. 3700–3714, Jul. 2015.
[24] M. J. Farooq, H. ElSawy, and M.-S. Alouini, "A stochastic geometry model for multi-hop highway vehicular communication," *IEEE Trans. Wireless Commun.*, vol. 15, no. 3, pp. 2276–2291, Mar. 2016.
[25] K. Feng and M. Haenggi, "A location-dependent base station cooperation scheme for cellular networks," *IEEE Trans. Commun.*, vol. 67, no. 9, pp. 6415–6426, Sep. 2019.
[26] N. Ross and D. Schuhmacher, "Wireless network signals with moderately correlated shadowing still appear Poisson," *IEEE Trans. Inf. Theory*, vol. 63, no. 2, pp. 1177–1198, Feb. 2016.
[27] A. D. Wyner, "The wire-tap channel," *Bell System Technical Journal*, vol. 54, no. 8, pp. 1355–1387, 1975.
[28] X. Yu, Q. Cui, and M. Haenggi, "SIR meta distribution for spatiotemporal cooperation in Poisson cellular networks," *IEEE Access*, vol. 7, pp. 73 617–73 626, 2019.